DEPARTMENT OF THE AIR FORCE

AIR UNIVERSITY

AIR FORCE INSTITUTE OF TECHNOLOGY

Wright-Patterson Air Force Base, Ohio

AFIT/GEO/ENP/88D-4

OPTICAL ACTIVITY AND ITS INFLUENCE ON PHOTOREFRACTIVE MATERIALS

THESIS

Richard J. Padden
Captain, USAF

AFIT/GEO/ENP/88D-4

Approved for public release; distribution unlimited

AFIT/GEO/ENP/88D-4

OPTICAL ACTIVITY AND ITS INFLUENCE ON PHOTOREFRACTIVE MATERIALS

THESIS

Presented to the Faculty of the School of Engineering
of the Air Force Institute of Technology
Air University
In Partial Fulfillment of the
Requirements for the Degree of
Master of Science in Electrical Engineering

Richard J. Padden, B.S.E.E.
Captain, USAF

December, 1988

Preface

The purpose of this study was to investigate the combined effects of optical activity and linear birefringence on photorefractive crystals. The relation of input-output intensity was determined. These results were discussed with regard to the operation and optimization of the conducting PRIZ.

The study focused on the crystal $Bi_{12}SiO_{20}$ (BSO) in order to correlate results with current experimental work at AFIT. The combination of optical activity and the photorefractive effect caused the crystal to be elliptically birefringent; this birefringence was modeled using Jones matrices for computer simulation. The simulation results showed that optical activity does have a noticeable effect, but for the application investigated the effect was small enough that it could be ignored. Recommendations were made to improve the quality of the output image of the PRIZ. More work should be performed in this area to investigate other applications of this phenomenon and also different crystal materials.

I would like to take this opportunity to thank my advisor, Dr. Ted Luke, for his guidance and patience during this research. I consider him to be more than an instructor; he is a true teacher. I also extend my appreciation to my thesis committee members, Drs. W. Bailey and W. Roh. Finally, I need to express my thanks, love, and appreciation to Tammy, Timmy, and Kevin, for putting up with me and supporting me throughout my stay at AFIT.

Richard J. Padden

Table of Contents

List of Figures

Abstract

This study characterized the effect of optical activity on the input-output properties of a photorefractive material. Optical activity is a material property that causes incident linearly polarized light to rotate as it travels through a crystal. The photorefractive effect causes a linear birefringence to develop in the crystal as a result of photoconductivity and the linear electro-optic effect The combination of optical activity and linear birefringence was investigated using two consistent representations: the Poincaré sphere and Jones matrices. The results showed that the combination of the two effects is a nonlinear superposition which results in an elliptically birefringent crystal.

The two representations were used to investigate the effects of optical activity in an imaging device called the PRIZ, which uses the optically active, photorefractive crystal BSO. The orientation of the eigenstates of the ⟨111⟩ PRIZ investigated are dependent on the direction, but not the magnitude, of the internal transverse electric field. Conversely, the amount of linear birefringence is dependent on only the magnitude of this field. Analysis of the input-output characteristics showed that for small values of linear birefringence close to the value of optical activity, the output intensity for elliptical birefringence was noticeably different from that of linear birefringence. Results also showed that elliptical input polarization exhibited directional filtering similar to that already reported for linear polarization, while circular input did not.

Trials were also run using the laboratory configuration of an analyzer biased to compensate for the optical rotation. The results showed that both linear and elliptical birefringence exhibited directional filtering and an asymmetric output intensity. The conclusions drawn from these results were that for the PRIZ imaging device, circular read beam input polarization is the best to use because it causes no

directional filtering. Also, for the PRIZ application of BSO discussed, the effects of optical activity result in a minor deviation from the case considering only the linear birefringence response. The recommendations from this study are to use circular input polarization for better imaging quality, and investigate other materials and applications involving optical activity.

OPTICAL ACTIVITY AND ITS INFLUENCE ON PHOTOREFRACTIVE MATERIALS

I. Introduction

Overview

Photorefractive materials have many applications of interest to the Air Force. When used as electro-optic spatial light modulators (ESLM), they can record two dimensional images and provide the high incoherent-to-coherent conversion rates of data necessary for fast optical processing. Bismuth Silicon Oxide ($Bi_{12}SiO_{20}$), or BSO, is a crystalline photorefractive material in wide use today.

The crystal symmetry of BSO is cubic, so it will behave isotropically when no forces are applied. Because of its molecular structure and the fact that it is non-centrosymmetric, BSO also exhibits a property known as optical activity. Optical activity causes the orientation of linearly polarized light, normally incident and traveling along a special direction of the crystal known as the optic axis, to rotate through some angle θ without the polarization state being changed.

When a longitudinal electric field is applied to a BSO crystal cut in the $\langle 111 \rangle$ orientation (see Appendix A), the linear electro-optic effect causes the crystal to become uniaxial. Also, if light of sufficient strength is incident on the crystal, the photorefractive effect will cause an induced transverse electric field. The transverse field will, in turn, cause the crystal to be biaxial, inducing a linear birefringence in the crystal.

Since photorefractive BSO is optically active as well as linearly birefringent, the combination of these two effects is of major interest. It turns out that the

combination is actually a nonlinear one, suggesting that these are not independent effects. Actually, this is not quite true, because the optical activity can be separated from the combination by measurement along an optic axis. This mixture of optical activity and linear birefringence results in a crystal having what is known as elliptical birefringence.

BSO analysis at AFIT has not considered the effect of optical activity on experimental results. This aspect needs to be addressed to help interpret experimental results already obtained and to guide future work with optically active materials.

Problem Statement

This thesis will characterize the effect of optical activity on the input-output properties of a photorefractive, optically active material by comparing a linearly birefringent crystal (ignoring optical activity) with an elliptically birefringent one (including optical activity). It will be restricted to the plane wave propagation of normally incident, polarized monochromatic light through a homogeneous, lossless medium.

The material to be investigated will be photorefractive BSO, and the crystal configuration will be the one tested at AFIT for the PRIZ spatial light modulator device. (PRIZ is a Russian acronym for image transformer.) The PRIZ device has been investigated by Gardner (3) at AFIT for imaging applications. Appendix A describes the laboratory setup, along with a discussion of the theory of operation for this imaging application.

The imaging operation of the PRIZ involves placing the crystal between a crossed linear polarizer-analyzer pair, where the analyzer provides an intensity variation of the image. This type of operation requires high image contrast, and unfortunately involves filtering that is dependent on the direction of the applied internal field (2:3850–3851).

Background

Optical Activity Optical activity causes the rotation of linearly polarized light along an optic axis. This is because the eigenstates of an optically active material are left- and right-circularly polarized. (Linear polarization can be represented by the sum of left and right circular polarization, so the linear light which travels through the crystal can be represented this way.) The circular birefringence of the material causes one of the circular modes to propagate faster than the other. When exiting the crystal, there are still two circular modes which combine to give linear polarization, but the difference in phase velocities causes the resultant linear polarization to be oriented at some other angle than it initially had (Figure 1) (5:309).

The amount of rotation of the polarization due to optical activity can be expressed in terms of the optical rotatory power, ρ, which is given in radians per unit thickness. The expression for the rotatory power is

$$\rho = \frac{\pi}{\lambda}(n_l - n_r) \tag{1}$$

where λ is the wavelength of incident light, and n_l and n_r are the indices of refraction associated with the left and right circularly polarized eigenstates, i.e. the normal modes for a purely optically active BSO crystal.

The optical rotatory power can be measured very easily using linearly polarized light and a linear analyzer crossed to the incident polarization. As the incident linear light travels along an optic axis, the orientation will be rotated. If no rotation occurred, then the crossed analyzer would extinguish the light. The analyzer then should be rotated from its crossed position to the point of extinguishing the output, thus giving the amount of rotation.

Rotatory power is easiest to measure in crystals with cubic symmetry, which have no preferred direction of optic axis. Even with the combination of other effects, such as linear birefringence, the rotatory power can be determined in all optically active crystals, provided a direction of an optic axis can be specified.

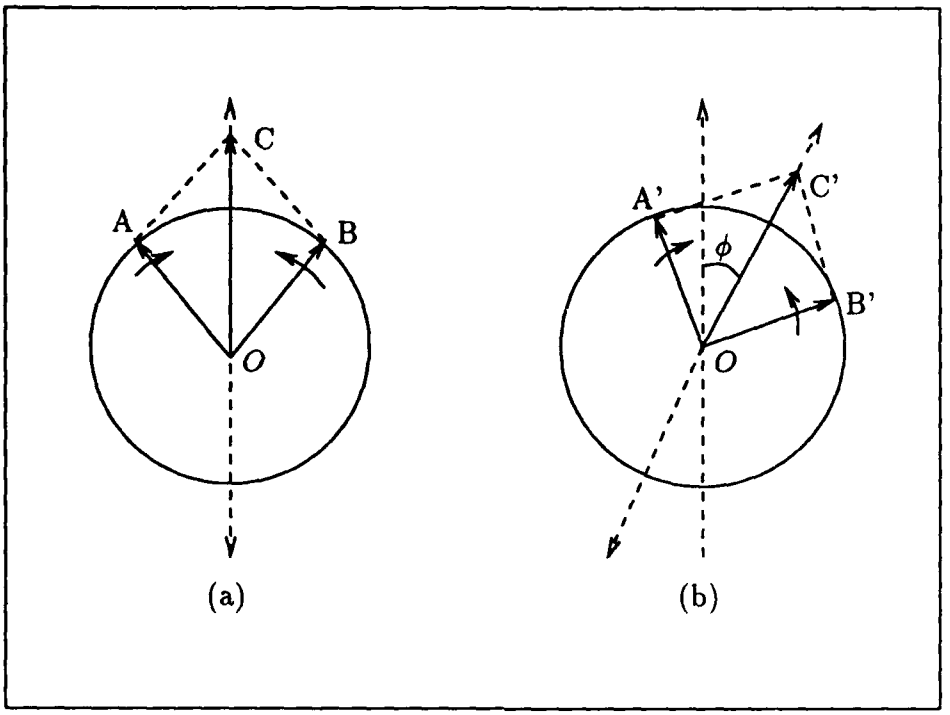

Figure 1. Optical Activity in a crystal along the optic axis (the optic axis direction is out of the page at O); (a) linear state C composed of circular states A and B at the entrance to the crystal (b) at the exit point, linear state C' is rotated because of different phase velocities with which A and B traveled.

Photorefractive Effect A photorefractive material uses photoconductivity and the linear electro-optic effect to change the material's index of refraction where incident light falls on it (12:789). The linear electro-optic effect arises from an externally applied electric field. Materials which exhibit this effect have third rank tensor components known as electro-optic coefficients, which vary according to crystal symmetry. These coefficients, when multiplied by the applied electric field, modify the

impermeability tensor b of the material, defined by

$$b = \begin{bmatrix} \frac{1}{n_1^2} & 0 & 0 \\ 0 & \frac{1}{n_2^2} & 0 \\ 0 & 0 & \frac{1}{n_3^2} \end{bmatrix} \tag{2}$$

where b is the inverse of the relative dielectric tensor, and the n's are the indices of refraction along the three crystallographic axes. The introduction of the electro-optic terms will cause b to be modified, in turn changing the indices of refraction.

A sufficient amount of photon energy incident on the crystal will cause electron-hole pairs to be excited from trap sites in the material, and then drift under the influence of the externally applied field. The charges will be retrapped in the crystal bulk, resulting in a space-charge field in the crystal. This field will then act in addition to the applied field, and cause local changes in the index of refraction (4:206).

Polarization The concept of polarization underlies many areas of this study, and must be discussed here in some detail. Linearly polarized light is a well understood and utilized concept. Somewhat less used are the ideas of circular and elliptical polarization, since they are harder to produce and are not as analytically convenient as linear polarization. However, circular and elliptical polarizations are very important because they describe the propagation of light through optically active, photorefractive crystals.

The polarization of the electric field vector $\vec{E}$ can be defined according to how the tip of the vector appears to rotate as it approaches an observer.

Elliptical polarization occurs when the tip of $\vec{E}$ appears to trace out an ellipse as it travels toward the observer. Alternatively, it can be defined as when the two orthogonal components making up the vector have a phase difference other than 0 or π radians.

Circular polarization is a special case of elliptical polarization. It occurs when the tip of $\vec{E}$ traces out a circle. It can also be defined by the vector components being out of phase by $\pm\pi/2$ *and* equal in magnitude. Both circular and elliptical polarization can rotate in either a left- or right-hand direction, depending on which component is leading the other.

Linear polarization is another special case of elliptical polarization. This occurs when the tip of $\vec{E}$ stays in a plane containing the direction of propagation, or when the vector components are 0 or multiples of π radians out of phase.

The phase velocity of light traveling through a crystal depends on both its polarization state and its direction of propagation. In general, the polarization of a wave traveling through the crystal will change. For a given direction of propagation, at most two waves of specific polarization, orthogonal to each other and the direction of propagation, can exist within the crystal. These waves have well-defined phase velocities and polarizations, and are known as the eigenstates, or normal modes, of the crystal. Any incident polarization that is identical to one of the eigenstates of the material will emerge unchanged (16:71–72).

The eigenstates are related to two independent indices of refraction that exist in *birefringent* materials. The concept of birefringence, or relative phase difference between the components of the light, stems from these two indices. Birefringence, like polarization, can be linear, circular, or elliptical, depending on the material properties. The most common type is linear birefringence, where the eigenstates of the crystal are two orthogonal, *linearly* polarized states. (The magnitude of the difference between the indices determines the amount of phase difference.) Likewise, circular birefringence occurs when the eigenstates of the crystal are two *circularly* polarized states. Two independent indices of refraction still exist, but each is now related to one of these circular states. Birefringence results from the phase difference between these two circular states. Finally, elliptical birefringence involves *elliptically* polarized eigenstates. These are two orthogonal states related to two indices of

refraction, and the same idea of phase difference applies.

Depending on the crystal symmetry, there are one, two, or an infinite number of directions in the crystal where the two indices of refraction are equal, causing no phase difference to occur. These directions are known as the optic axes. *Uniaxial* crystals have one optic axis, *biaxial* crystals have two, and *isotropic* crystals have an infinite number. Because the indices of refraction are equal along the optic axis direction in a linearly birefringent material, incident polarization in this direction will not change form.

Approach

This study will address the problems of characterizing elliptically birefringent BSO and improving the performance of the PRIZ imaging device.

Chapter II will look at the mathematical representation of an elliptically birefringent crystal. Two relatively easy, yet still very accurate, methods of representation will be discussed.

The first method is known as the Poincaré sphere. This is a sphere of unit radius which represents every type of polarization through points on the sphere. Propagation of polarization through birefringent crystals is handled by merely rotating the sphere about the axis containing the eigenstates (13:2,12). The Poincaré sphere is extremely easy to use and gives a good intuitive feel for what happens physically to light after it propagates through an elliptically birefringent material.

The second method of representation is known as the Jones matrices. These matrices were developed to represent the optical elements of a system, so that computations involving polarized light passing through a system would merely be a matter of multiplying matrices (6:671). A single Jones matrix can also represent the different properties of a crystal, such as optical activity and linear birefringence. The Jones matrix method will be used to analyze linear and elliptical birefringence, due to its ease of calculation and parameterization.

Chapter III analyzes variations in output intensity for linearly and elliptically birefringent cases relating to the PRIZ configuration. Elliptically birefringent BSO will be shown to have some marked differences from the linearly birefringent case. Some previously unexplained experimental results will also be shown to compare very well with the results of computer simulation.

Finally, Chapter IV provides the conclusions resulting from the analysis. It also includes some recommendations for experimental procedures which could be applied to operations involving the PRIZ device previously described.

II. Elliptical Birefringence

This chapter will discuss two separate but consistent methods of representing a crystal which exhibits both optical activity and linear birefringence (BSO in particular). The two ways of representing this elliptically birefringent crystal include the Poincaré sphere and Jones matrices. The Poincaré sphere will be addressed first in order to give an intuitive feel for the effect an anisotropic material has on polarization. The Jones matrix method will then be used to provide a matrix expression for the elliptically birefringent crystal; the matrix will allow computational ease and analytical convenience. (Appendix B contains a description of the mathematical expression for this crystal in terms of Maxwell's equations; the two methods described in this chapter are consistent with the solution described in Appendix B.)

Poincaré Sphere

The Poincaré sphere was conceived by Henri Poincaré about 1892 to conveniently represent polarized light. Elliptically polarized light is the most general case of polarization. Therefore, a polarization state can be described by the orientation of the major axis of the ellipse, and the ellipticity or ratio of the minor axis b to the major axis a (Figure 2) (13:5). The orientation of the major axis can be specified by an angle ϕ from the horizontal axis, while the ellipticity can be defined by an angle ω, such that $\tan\omega = b/a$. Thus, any state of polarization can be completely described by ϕ and ω, where ϕ ranges from 0 to π, and ω ranges from $-\pi/4$ to $\pi/4$. The states of polarization can be represented on a sphere of unit radius having latitude of 2ω and longitude of 2ϕ. Therefore, the surface of the sphere is completely covered as 2ϕ goes from 0 to 2π, and 2ω goes from $-\pi/2$ to $\pi/2$ (Figure 3). All linear polarization states are located on the equator, while left and right circularly polarized states are at the opposite poles. Also, the two states on any axis through the origin are orthogonal, including opposite senses of rotation (13:2).

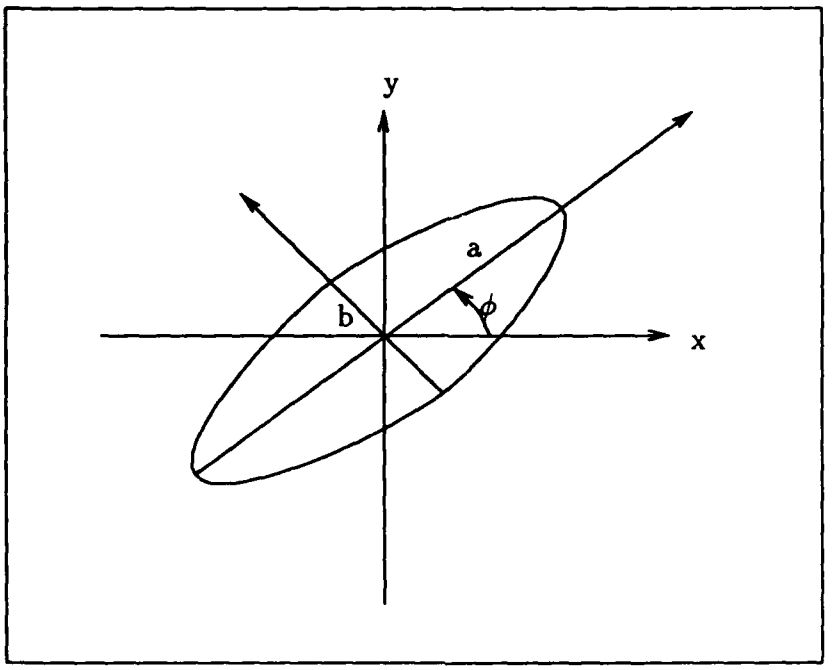

Figure 2. Elliptically polarized light

The Poincaré sphere is well suited to determining the change in polarization of light passing through an anisotropic crystal. For example, a linearly birefringent crystal will have two linear, orthogonal eigenstates. These states would be depicted on the Poincaré sphere by H and V for horizontal and vertical, respectively (Figure 3). If a linear polarization other than these two is incident, the two components will undergo a phase difference δ, generally resulting in elliptical light being produced. This is easily predicted on the sphere by starting at the point of the incident light P_0 and rotating it counterclockwise about the HV axis (if H is the faster state) a value of δ; the resulting point P_1 is the emerging polarization state.

Likewise, if a purely optically active crystal causes a phase difference δ between the left and right circular modes, the incoming polarization will be rotated about the polar axis by δ. Thus, only the orientation of the polarization will change, while the ellipticity remains the same (13:6).

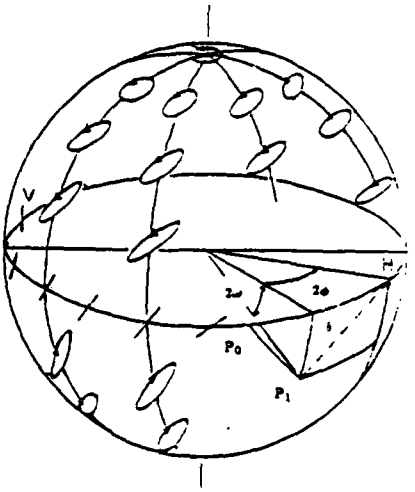

Figure 3. Poincaré Sphere

When determining the properties of an elliptically birefringent crystal, it is helpful to think of this material as being composed of alternating infinitesimal layers of strictly optical activity and strictly linear birefringence. (Although this should not be assumed for a rigorous solution, it nevertheless is a good approximation.) Suppose now that the two eigenstates of the linearly birefringent layer are represented by M and N in Figure 4, where M is the fast axis. Given that the linear birefringence

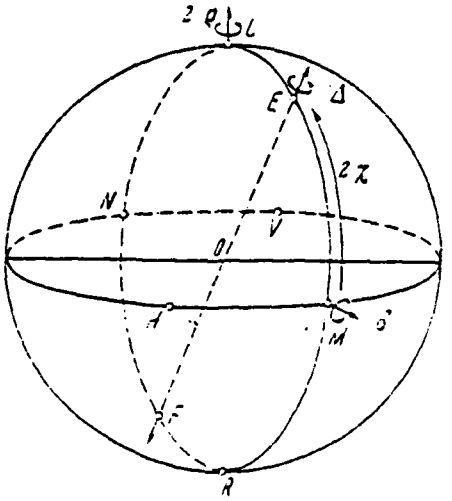

Figure 4. Normal modes for elliptically birefringent crystal

is δ and the optical rotation is ρ, the effect of going through both elements is a rotation by δ about MN, followed by a rotation of 2ρ about LR. Since these layers are infinitesimally thick, the order of the rotations doesn't matter. Furthermore, the sum of the infinitesimal rotations is a vector addition. If the resultant is defined as Δ, then

$$\Delta^2 = \delta^2 + (2\rho)^2 \tag{3}$$

This equivalent rotation Δ is about an axis EF, located in the plane of LR and MN, and situated at the angle 2χ from MN given by

$$2\chi = \arctan \frac{2\rho}{\delta} \tag{4}$$

Thus, for an optically active, linearly birefringent crystal, the normal modes are the elliptical states represented by E and F. The crystal is therefore elliptically birefringent (13:11–12).

The Poincaré sphere is useful for determining the input-output polarization characteristics for crystals, but the major work of this study is in determining intensity variations of the output. As a result, operations involving Jones matrices will now be required. A discussion of these matrices is therefore in order.

Jones Matrices

The Jones calculus was developed to represent each element of an optical system in terms of a matrix M. The electric vector $\vec{E}$ of the incident light on this element is defined by

$$\vec{E} = \begin{bmatrix} X \\ Y \end{bmatrix} \tag{5}$$

where X and Y are the two complex transverse components of the vector. Each M matrix is defined as a 2×2 element matrix so that the electric vector $\vec{E}'$ emerging from the optical element is

$$\vec{E}' = \mathrm{M}\vec{E} \tag{6}$$

The method of Eq(6) describes the states of polarization only between optical elements of a system, since M defines the overall behavior of the element. In order to deal with elements containing a number of different optical effects, Jones developed an approach which allowed the state of polarization to be determined at every point within the element. This approach used what he called N matrices (6:672), and is described as follows.

Consider the matrix $M_{z,z'}$, which describes the properties of a thin layer of an optical element between z and z'. From Eq(6),

$$\vec{E}_{z'} = M_{z,z'}\vec{E}_z \tag{7}$$

The N matrix at the z coordinate represents an infinitesimally thick layer of the element defined by

$$N_z \equiv \lim_{z' \to z} \frac{M_{z,z'} - I}{z' - z} \tag{8}$$

where I is the identity matrix. If M_z is the matrix of the element up to the coordinate z, then

$$M_{z,z'} = M_{z'}M_z^{-1} \tag{9}$$

Substituting Eq(9) into Eq(8) gives

$$N \equiv (dM/dz)M^{-1} \tag{10}$$

where the subscript z is no longer needed. In determining a series relation for M in terms of N, successive differentiation of Eq(10) is used to give

$$M = \exp(Nz) \tag{11}$$

To represent an arbitrary homogeneous crystal as a combination of simple properties, consider that an M_s matrix of a very thin slice of the crystal is very close to the identity matrix. The multiplication order of these thin M_s slices necessary to approximate the crystal M matrix is thus immaterial. Each of these M_s matrices

can be represented by a product of factors which relate to simple optical properties. The N matrices are a good way of representing these properties.

Jones defined eight unique types of crystalline behavior which could be represented by N matrices. These include phase retardation, absorption, rotation, linear birefringence, and dichroism. If each of these eight matrices are defined as N_k with related thicknesses τ_k, then $\bar{N}$ is a weighted average of all the N_k's:

$$\bar{N} \equiv \frac{\sum_k N_k \tau_k}{\sum_k \tau_k} \tag{12}$$

The M_s matrix may be given by

$$M_s = I + \bar{N}\tau + O(\tau^2) \tag{13}$$

where τ is the total thickness of the sandwich of eight properties, and $O(\tau^2)$ is a second order term in τ.

Now consider a number q of these M_s sandwiches piled together. The M matrix of the pile is

$$M = M_s^q \tag{14}$$

As the number q increases without limit, the thickness τ goes to zero. So the limit of Eq(14), after substituting in Eq(13), must be calculated as τ goes to zero. The result leads to

$$M = \exp(T_N z) \begin{bmatrix} \cosh Q_N z + \frac{1}{2}(n_1 - n_2)\frac{\sinh Q_N z}{Q_N} & n_4 \frac{\sinh Q_N z}{Q_N} \\ n_3 \frac{\sinh Q_N z}{Q_N} & \cosh Q_N z - \frac{1}{2}(n_1 - n_2)\frac{\sinh Q_N z}{Q_N} \end{bmatrix} \tag{15}$$

where n_1, n_2, n_3, and n_4 are elements of the N matrix; T_N is the half-trace of N defined as $\frac{1}{2}(n_1 + n_2)$; Q_N is the discriminant of N defined as $(\frac{1}{4}(n_1 - n_2)^2 + n_3 n_4)^{1/2}$, and $\bar{N}$ is substituted for N (6:676).

Jones made a simplification by assuming that the eight slices of the sandwich were all of equal thickness, and the eight simple properties were represented by Θ matrices. $\bar{N}$ is then equal to the sum of all the Θ matrices which apply to the crystal.

The Θ matrices for optical rotation and linear birefringence are given as

$$\Theta_{OR} = \rho \begin{bmatrix} 0 & -1 \\ 1 & 0 \end{bmatrix} \tag{16}$$

where ρ is the optical rotatory power, and

$$\Theta_{LB} = \xi \begin{bmatrix} i & 0 \\ 0 & -i \end{bmatrix} \tag{17}$$

where ξ is one half of the relative phase retardation per unit thickness (6:682). The $\bar{\mathrm{N}}$ matrix for the linear birefringent case is then

$$\bar{\mathrm{N}}_{LB} = \begin{bmatrix} i\xi & 0 \\ 0 & -i\xi \end{bmatrix} \tag{18}$$

Substitution of Eq(18) into Eq(15) gives

$$\mathrm{M}_{LB} = \begin{bmatrix} e^{i\xi z} & 0 \\ 0 & e^{-i\xi z} \end{bmatrix} \tag{19}$$

The $\bar{\mathrm{N}}$ matrix for the combination of optical activity and linear birefringence is

$$\bar{\mathrm{N}}_{OA+LB} = \begin{bmatrix} i\xi & -\rho \\ \rho & -i\xi \end{bmatrix} \tag{20}$$

and substitution into Eq(15) gives

$$\mathrm{M}_{OA+LB} = \begin{bmatrix} \cos(\Gamma z) + \frac{i\xi}{\Gamma}\sin(\Gamma z) & -\frac{\rho}{\Gamma}\sin(\Gamma z) \\ \frac{\rho}{\Gamma}\sin(\Gamma z) & \cos(\Gamma z) - \frac{i\xi}{\Gamma}\sin(\Gamma z) \end{bmatrix} \tag{21}$$

where $\Gamma = (\xi^2 + \rho^2)^{1/2}$. Since ξ is one half the linear birefringence δ, Γ is related to Δ of Eq(3) by

$$|\Delta| = 2\Gamma \tag{22}$$

In summary, the representation of an elliptically birefringent crystal was developed. An electromagnetic description was initially used to derive the phase difference

Δ between the eigenstates of this type of crystal. The Poincaré sphere was used to show that the eigenstates are elliptically polarized, making the crystal elliptically birefringent. The Jones matrices were then discussed, where the optical properties of the crystal were represented in terms of an M matrix composed of a product of matrices depicting many slices of the crystal. These slices were in turn composed of eight N matrices; an $\bar{N}$ matrix, a weighted average of the eight N matrices, was made up of a sum of eight Θ matrices. The Θ matrices define unique optical behavior. Thus, an M matrix for an elliptically birefringent crystal was developed.

With the results of Eq(21), it is now possible to analyze the behavior of elliptically birefringent BSO in relation to the PRIZ operation. The next chapter will compare this case with the linearly birefringent case of Eq(19), in order to determine the effect of optical activity.

III. Comparison of Elliptical and Linear Birefringence

This chapter will discuss the configuration used to represent the PRIZ imaging device in terms of Jones matrices. Related discussions will include polarizers, orthogonal analyzers, and variables and parameters used in the analysis. Results of analysis using the commercial software package MathCAD will be presented and discussed. Finally, analysis related directly to experimental results will be given.

As previously mentioned about the PRIZ, the read beam is essential to the imaging operation of the device. Recall that the read beam is usually linearly polarized; this, however, is not a necessity. Although circular and elliptical polarization are harder to produce, the luxury of computer analysis allows the investigation of both these cases to see if the benefits outweigh the hardships.

Recall also that the imaging operation requires an analyzer orthogonal to the polarizer to give intensity variations of the image. The importance of the polarizer-analyzer pair suggests a detailed discussion here.

Polarizer-Analyzer Pairs

Producing linear light is very simple using sheet polarizers, which are easy to make and use. A circular polarizer can be made using a linear polarizer and a quarter wave plate aligned so the transmission axis of the polarizer bisects the fast and slow axes of the quarter wave plate. This causes the two emerging vector components to be of equal magnitude and $\pi/2$ out of phase (14:39). Elliptically polarized light can also be produced using a linear polarizer and quarter wave plate (13:4). The ellipticity of the polarization ellipse is determined by the angle of the transmission axis of the linear polarizer, and the orientation of the ellipse is determined by the orientation of the quarter wave plate. (In fact, there are an infinite number of combinations of the linear polarizer and wave plate, so that the selection of a reference coordinate system is important in producing the elliptical light.) The sense of rotation of the

polarization depends on the relative positions of the fast and slow axes to the incident linear polarization (Figure 5).

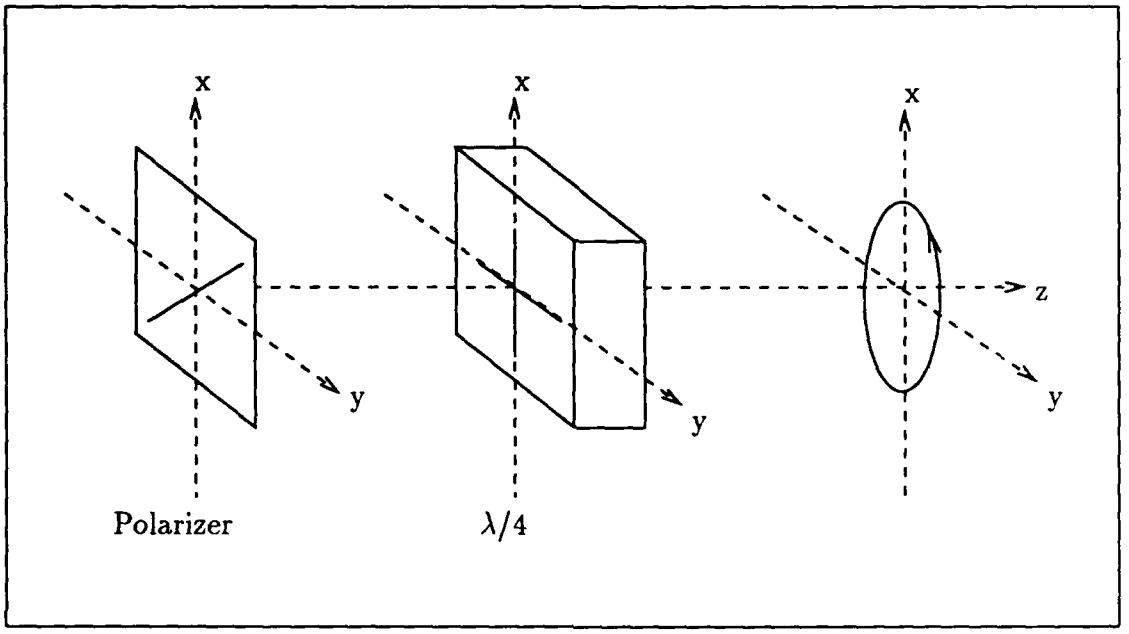

Figure 5. Elliptical polarizer consisting of linear polarizer and quarter wave plate

A linear analyzer can be made orthogonal to the linear polarizer by simply rotating the transmission axis of the analyzer by $\pi/2$ with respect to the polarizer transmission axis. Then if nothing happens to the beam in between the pair, there will be a total extinction of the light at the output. It might be assumed that an orthogonal elliptical analyzer could be set by a simple rotation of $\pi/2$ also. However, the orthogonality must include an opposite sense of handedness. Using the Jones matrices, consider the eigenvectors of the elliptical polarizer to be

$$\begin{bmatrix} m \\ n \end{bmatrix} \text{ and } \begin{bmatrix} -n^* \\ m^* \end{bmatrix} \tag{23}$$

where m and n are complex components, in general. The Jones matrix of the polar-

izer is then

$$\begin{bmatrix} mm^* & mn^* \\ m^*n & nn^* \end{bmatrix} \tag{24}$$

so that the first state of Eq(23) would emerge from the polarizer unchanged, except for a constant, but the second state would be extinguished (Eq(25)) (14:167).

$$\begin{aligned} (mm^* + nn^*) \begin{bmatrix} m \\ n \end{bmatrix} &= \begin{bmatrix} mm^* & mn^* \\ m^*n & nn^* \end{bmatrix} \begin{bmatrix} m \\ n \end{bmatrix} \\ \begin{bmatrix} 0 \\ 0 \end{bmatrix} &= \begin{bmatrix} mm^* & mn^* \\ m^*n & nn^* \end{bmatrix} \begin{bmatrix} -n^* \\ m^* \end{bmatrix} \end{aligned} \tag{25}$$

The matrix of an orthogonal elliptical polarizer, which would pass the second state of Eq(23) and extinguish the first, is

$$\begin{bmatrix} nn^* & -mn^* \\ m^*n & mm^* \end{bmatrix} \tag{26}$$

The matrix of Eq(26) causes an interchange of major and minor axes with Eq(24), while also providing an opposite sense of rotation. The elliptical polarizer case degenerates directly to the circular polarizer where the magnitude of m and n are now equal. An interesting fact about the orthogonal circular polarizers is that relative orientation to each other doesn't matter, whereas the orientation between the elliptical polarizers does because of the interchanging of the major and minor axes.

Variables and Parameters

The next area to discuss is variables and parameters used for the analysis. It is interesting that for the PRIZ configuration of BSO the orientation of the eigenstates is a function of the direction of the transverse internal field. This dependence is a key to the imaging results of the crystal, so the orientation of the eigenstates shall be one of the variables of interest, rotating from 0 through 2π.

The following discussion of the orientation of eigenstates will at first deal with linear birefringence; this is done to use the index ellipsoid method to simplify the explanation. The direct extension of these results to elliptical eigenstates will be demonstrated using the Poincaré sphere.

Recall the impermeability tensor b mentioned in Chapter I. If a finite internal field is applied to the crystal, this tensor is modulated:

$$b(\vec{E}) = b + \Delta b \tag{27}$$

where $\Delta b_{ij} = \sum_k r_{ijk} E_k$, E_k are the components of the internal electric field, and r_{ijk} are the electro-optic coefficients previously mentioned. For BSO, the only nonzero r elements are $r_{231} = r_{132} = r_{123}$. The tensor for $b(\vec{E})$ becomes

$$b(\vec{E}) = \begin{bmatrix} \frac{1}{n^2} & \Delta b_{12} & \Delta b_{13} \\ \Delta b_{12} & \frac{1}{n^2} & \Delta b_{23} \\ \Delta b_{13} & \Delta b_{23} & \frac{1}{n^2} \end{bmatrix} \tag{28}$$

The index ellipsoid equation related to Eq(28) is

$$\sum_i \sum_j b_{ij}(\vec{E}) x_i x_j = 1 \tag{29}$$

Equation (29) is the index ellipsoid equation for the (x_1, x_2, x_3) coordinate system, which here represents the principal coordinate axes. But the PRIZ device is oriented in the (111) coordinate system, represented here by (x'_1, x'_2, x'_3). The transformation of Eq(29) into this new coordinate system leads to

$$\sum_i \sum_j b'_{ij}(\vec{E}) x'_i x'_j = 1 \tag{30}$$

where $b'_{ij}(\vec{E})$ is the transformation of $b_{ij}(\vec{E})$ into the primed coordinate system.

In this new coordinate system, x'_3 is the direction of propagation, so setting it to zero gives

$$b'_{11}(x'_1)^2 + 2b'_{12}(x'_1 x'_2) + b'_{22}(x'_2)^2 = 1 \tag{31}$$

which is an equation of a rotated ellipse. This ellipse in fact contains all the information necessary to describe the propagation of plane waves through the linearly birefringent crystal. The lengths of the major and minor semi-axes represent the indices of refraction for the two normal modes of propagation, while the directions of the axes indicate the polarization orientations of these two modes. It turns out that, given b as a function of the internal field, the orientation of the normal modes with respect to the x'-coordinate system is

$$\alpha = \frac{1}{2}\left(\theta + \frac{\pi}{2}\right) \tag{32}$$

where α is the angle between the direction of the normal modes and the (x_1', x_2') axes, and θ is the angle between the x_1' axis and the transverse component E_t of the internal electric field (Figure 6) (9:649). The results of Eq(32) show that the orientation of the eigenstates are directly related to the direction of the internal transverse electric field; it also shows that the magnitude of the field does not affect the eigenstates.

The extension of Eq(32) to elliptical eigenstates can be done using the Poincaré sphere. Recall from Figure 4 that the eigenstates of an elliptically birefringent crystal are located in the plane containing the axes for optical rotation and linear birefringence. Now considering Eq(32), as the direction θ of the internal field rotates through 2π radians, the orientation α of the eigenstates will rotate through 4π. For linearly birefringent crystals, this is shown on the Poincaré sphere by following the polarizations on the equator around the sphere. For the elliptical birefringence, the eigenstates are in the same longitude as the linear states, so the orientation of the major axis of the ellipse is the same as the orientation of the linear eigenstate. Equation (32), then, holds for elliptical birefringence also, where α is now the angle between the major axes of the normal modes and the (x_1', x_2') axes (Figure 7).

The retardation of the two linear normal modes for the PRIZ orientation was

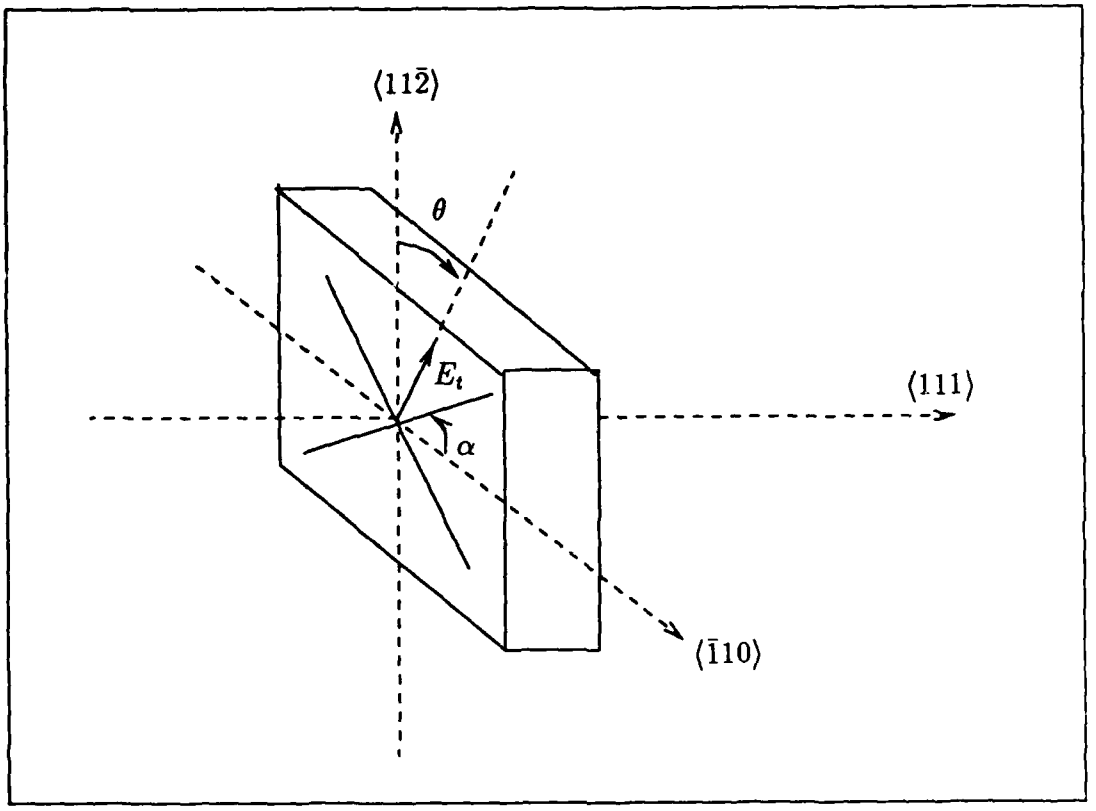

Figure 6. Orientation of eigenstates α is a function of direction θ of internal transverse field E_t

given by Owechko and Tanguay (9:650) as

$$\delta = \frac{2\pi}{\lambda}(2/3)^{1/2} n^3 r E_t d \tag{33}$$

where n is the refractive index of BSO, r is the electro-optic coefficient, E_t is the magnitude of the induced transverse field, and d is the thickness of the crystal. The interesting thing to note here is that the retardation is a function of the magnitude only of the transverse electric field, not the field direction. The other variable that will be considered, then, is the amount of birefringence induced in the photorefractive crystal by light incident on the crystal.

Parameters used in the first part of the analysis (i.e. varying the orientation

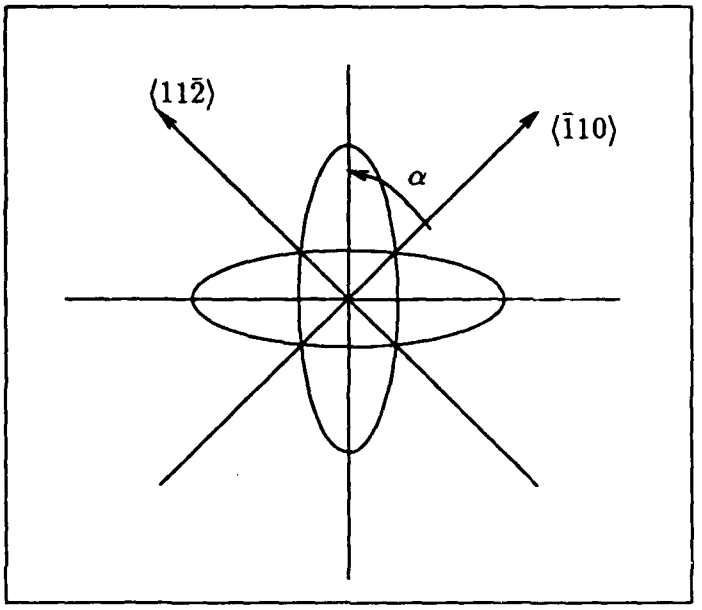

Figure 7. Orientation α of elliptical eigenstates

of the eigenstates) will include different forms and orientations of input read beam polarization, the amount of the linear birefringence δ, and the amount of optical activity ρ. Parameters used in the second part of the analysis (i.e. varying the linear birefringence) will be discussed after results from the first part of the analysis are presented.

Because the form of the read beam polarization is not restricted, the input polarizations investigated will include linear, circular, and elliptical. This brings up a question of what coordinate system to use in terms of the input polarization. Since the Jones matrices of Eqs(19) and (21), representing linear and elliptical birefringence, are referenced in the crystallographic coordinate system, this system is a logical choice for use as a reference for the entire train of optical elements.

Linear read beam polarization will be the first type investigated. Since optical activity is usually ignored, the crystal itself is assumed to be linearly birefringent; the incident polarization is of the same form as the eigenstates. To create an analogous

situation for elliptical birefringence, the case of incident elliptical read beam polarization will contain elliptical eigenstates. These eigenstates are determined from the eigenvalue relation involving the matrix of Eq(21). Diagonalization of this matrix leads to the two eigenstates

$$\begin{pmatrix} i\rho \\ \Gamma - \xi \end{pmatrix} \qquad \text{and} \qquad \begin{pmatrix} -i\rho \\ \Gamma + \xi \end{pmatrix} \tag{34}$$

So input polarization of either of these forms would emerge from the crystal represented by Eq(21) unchanged in magnitude and phase difference (15:158–159).

The linear birefringence in Eq(21) is represented by ξ. In fact, this is actually one half the relative phase difference δ between the linear eigenstates. In most applications involving the linear electro-optic effect, voltages are applied so that δ rarely exceeds π radians (a half wave plate). Therefore, in this study, δ will be considered to have values of π or less. Because ξ is per unit thickness, and the experimental crystal is 1/2 mm thick, the values of ξ will represent δ. So the values of ξ used will be π, $2\pi/3$, $\pi/2$, and $\pi/4$. These values, while not all inclusive, are expected to provide a good representative sample of results reflecting practical use.

The final parameter used is the amount of optical activity ρ. The value of ρ is dependent on the wavelength of the incident polarization and is given per unit thickness. For BSO, the amount of optical activity for 633nm wavelength light is $\rho = 22°/\text{mm}$ (10:154). In the experimental device, a helium-neon laser with wavelength of 633nm is used for the read beam. To relate the analysis to experimental values, the value of ρ will therefore be set to $\pi/9$, or $20°/\text{mm}$. A value of $\pi/4.5$, or $40°/\text{mm}$, will also be used for comparison.

Results for Orientation of Eigenstates

System Configuration and Results The system configuration of Jones matrices equivalent to the PRIZ set-up can be thought of as

$$E' = AR'MRE \tag{35}$$

where E and E' are the electric field column vectors representing the input and output polarization of the light, respectively; R and R' are rotation matrices which transform the incoming polarization into the α coordinates and back out into the crystallographic coordinates; M is the matrix of the crystal itself; and A is the orthogonal analyzer. The rotation matrices are given as

$$R = \begin{bmatrix} \cos\alpha & -\sin\alpha \\ \sin\alpha & \cos\alpha \end{bmatrix} \qquad \text{and} \qquad R' = \begin{bmatrix} \cos\alpha & \sin\alpha \\ -\sin\alpha & \cos\alpha \end{bmatrix} \tag{36}$$

for the situation as shown in Figure 6. The intensity of the output polarization is the main concern for the imaging device. The intensity I is found from

$$I = |E'|^2 \tag{37}$$

which is a matter of squaring the two components of E' and adding them to give the intensity (neglecting the scale factor) for the related value of α.

A factor to consider for image quality is the concept of contrast. Contrast as used here will be defined by the difference between the maximum intensity achieved for a specific value of the induced transverse field (which is related to ξ), and the maximum intensity achieved for no induced transverse field. It is desired that the baseline for the intensity be zero for zero internal electric field (Figure 8).

Linear Input Polarization For the case of input linear polarization, the functional diagram is shown in Figure 9. The term E in Eq(35) actually represents the state of the light immediately after going through the polarizer, so that travel through the entire system is given by

$$\begin{bmatrix} E'_{x_1} \\ E'_{x_2} \end{bmatrix} = \begin{bmatrix} \cos^2\gamma & \sin\gamma\cos\gamma \\ \sin\gamma\cos\gamma & \sin^2\gamma \end{bmatrix} \begin{bmatrix} \cos\alpha & \sin\alpha \\ -\sin\alpha & \cos\alpha \end{bmatrix} M \begin{bmatrix} \cos\alpha & -\sin\alpha \\ \sin\alpha & \cos\alpha \end{bmatrix} \begin{bmatrix} \cos\beta \\ \sin\beta \end{bmatrix} \tag{38}$$

β is the angle of the transmission axis of the polarizer with x'_1; $\gamma = \beta + \pi/2$; and M is either the linearly birefringent matrix Eq(19), or the elliptically birefringent matrix Eq(21).

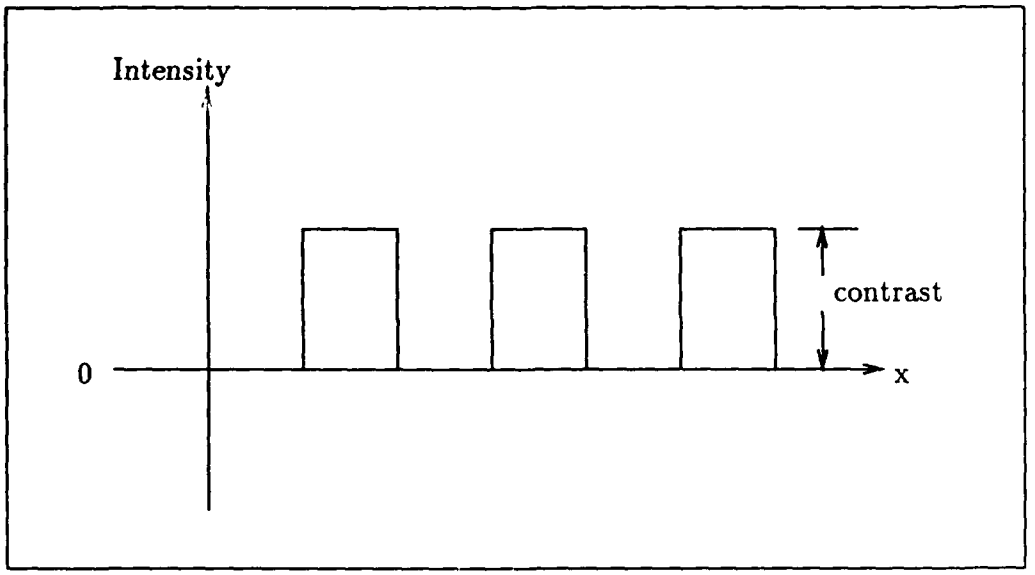

Figure 8. Intensity contrast

To simplify the computations and to simulate the experimental procedure, the orientation of the input linear polarization will be parallel to the x_1' axis. This requires $\beta = 0$, and $\gamma = \pi/2$. The thickness z in Eqs(19) and (21) is considered to be 1/2 mm, the thickness of the experimental crystal.

The expected intensity results using linearly polarized input can be found by examining the scenario of Figure 10. The linearly birefringent crystal, with its orthogonal linear eigenstates, is represented in Figure 10(a) along with the linearly polarized input E_{in}, and a linear analyzer orthogonal to E_{in}. The elliptically birefringent crystal, with its orthogonal elliptical eigenstates, is represented in Figure 10(b) along with the same input- analyzer setup.

The linear birefringence scenario, Figure 10(a), will be examined first. If the linear eigenstates are aligned with the crystallographic axes, then E_{in} will be parallel to one of these eigenstates, and pass unchanged through the crystal. Upon exiting the crystal, the polarization will be completely crossed with the direction of the analyzer, causing extinction of the output intensity. This is expected to happen as

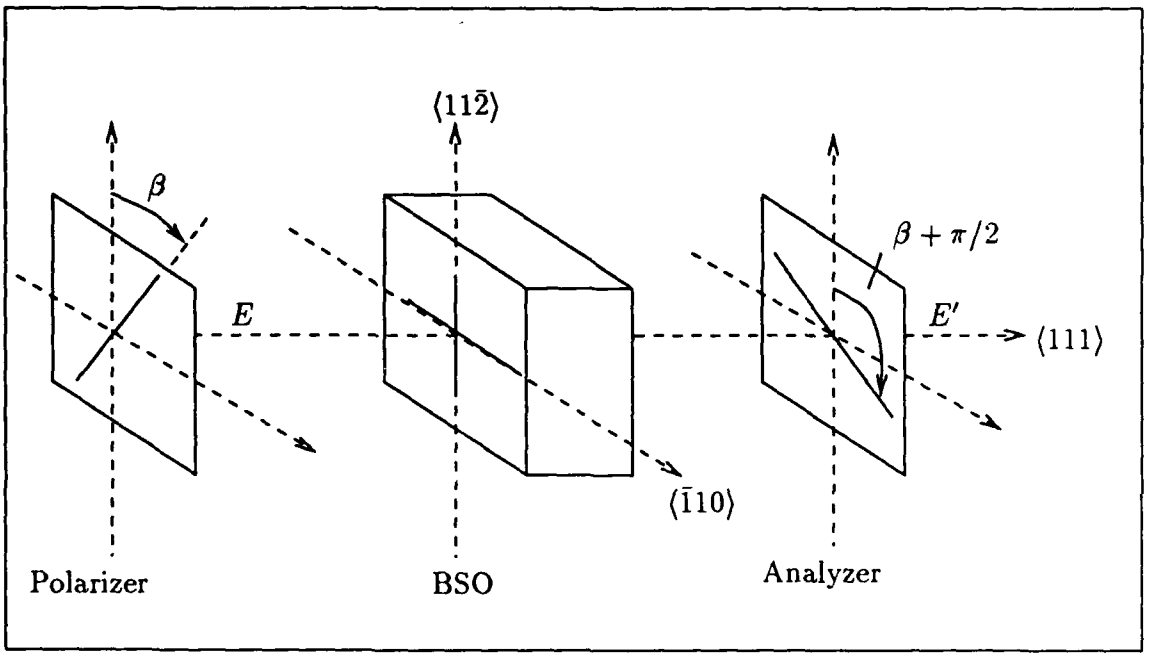

Figure 9. Test configuration for linear polarization

α goes through multiples of $\pi/2$.

For the elliptical birefringence scenario, Figure 10(b), the linear input polarization will never be passed unchanged (except for $\alpha = \pi/4$ in a half wave plate) because it cannot match itself to one of the elliptical eigenstates. It is expected, then, that a total extinction of the intensity output is not possible for this scenario.

For either scenario, the output intensity is maximum when the eigenstates are situated at $\pi/4$ to the crystallographic axes. This is determined by using the Poincaré sphere to find the orientation of the output polarization of the crystal for each orientation of the eigenstates. The magnitude of the output polarization component parallel to the analyzer transmission axis determines which orientation of the eigenstates causes the maximum intensity output.

The results shown in Figure 11 are for the values $\xi = \pi$ and $\rho = \pi/9$. The

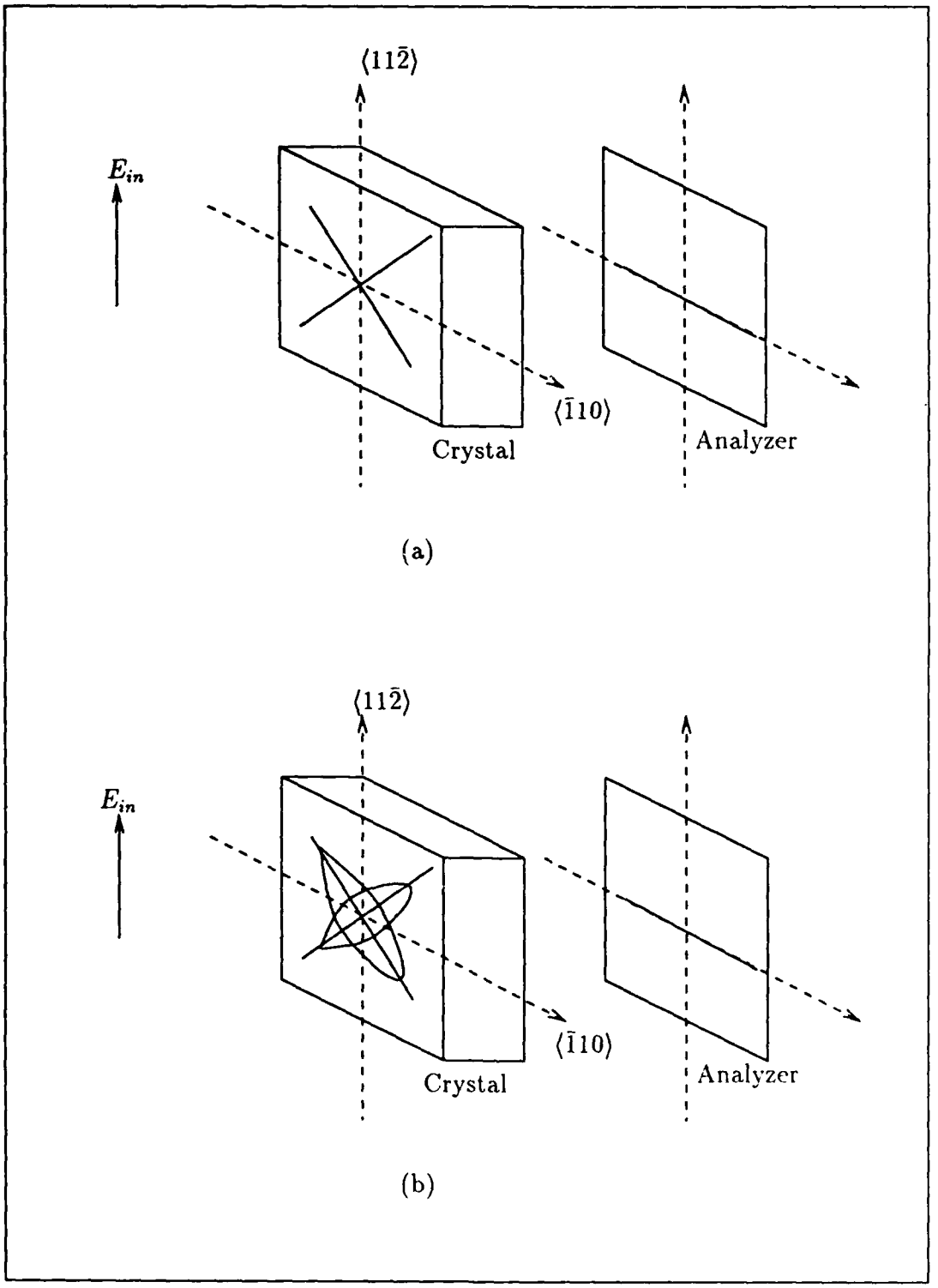

Figure 10. Linear input for (a) linear eigenstates and (b) elliptical eigenstates

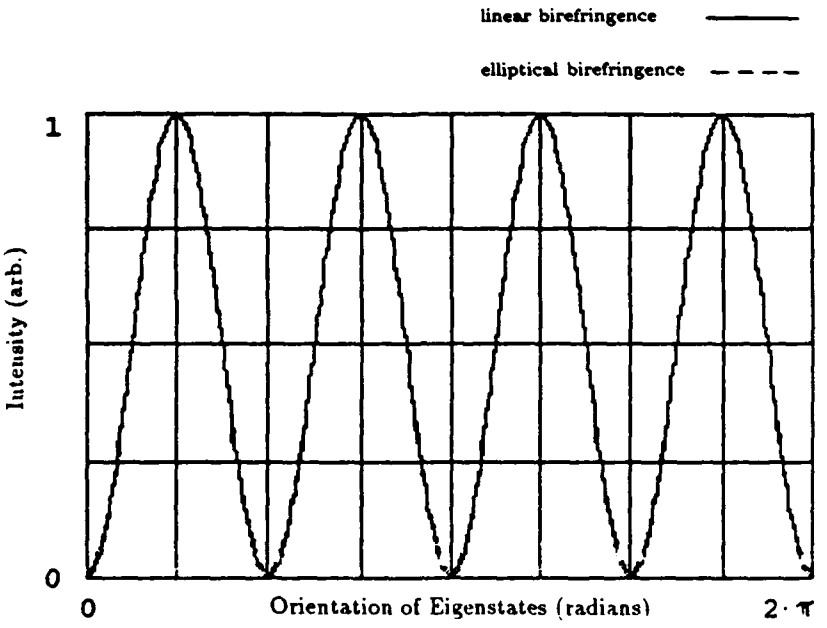

Figure 11. Intensity profile for linear input with $\xi = \pi$ and $\rho = \pi/9$

maximum intensity for this case goes to unity because the crystal is acting as a half wave plate. When the eigenstates are at $\alpha = \pi/4$, the incident linear polarization will be rotated $\pi/2$. The output polarization is then parallel to the analyzer, which passes all of the light.

The results of Figure 11 also show the points where the linear birefringence leads to a total extinction of the light while the elliptical birefringence doesn't. The two curves shown here are very similar because the amount of optical activity is small relative to the amount of linear birefringence.

The results shown in Figures 24–30 in Appendix D indicate how decreasing the amount of linear birefringence in relation to the optical activity causes pronounced separations of the two curves. They also show how the maximum intensity of these curves decreases with decreasing linear birefringence.

An interesting thing to note in the results of the linear input polarization cases

is that the output intensity varies as $\sin^2 \alpha$. This is the directional filtering problem mentioned in Chapter I. For example, an input image of a circle, with uniform photon energy for all directions, will actually have an output image of continually varying intensity. There is even an axis along which extinction (or near-extinction) occurs. This results in poor imaging quality.

Circular Input Polarization The configuration for input circular polarization is similar to Figure 9, except for the polarizer and analyzer now being circular and orthogonal. The equivalent system in terms of Jones matrices is

$$\begin{bmatrix} E'_{x_1} \\ E'_{x_2} \end{bmatrix} = \begin{bmatrix} bb^* & -ab^* \\ -a^*b & aa^* \end{bmatrix} \begin{bmatrix} \cos\alpha & \sin\alpha \\ -\sin\alpha & \cos\alpha \end{bmatrix} M \begin{bmatrix} \cos\alpha & -\sin\alpha \\ \sin\alpha & \cos\alpha \end{bmatrix} \begin{bmatrix} a \\ b \end{bmatrix} \quad (39)$$

where $a = \cos(\pi/4)$, $b = i\sin(\pi/4)$, and M again is either Eq(19) or Eq(21).

The scenarios for the circular input polarization are shown in Figures 12(a) and 12(b). The analyzers in these cases are orthogonal to the input polarization because they would completely pass circular polarization of the opposite handedness to the input polarization.

By using the Poincaré sphere, the output characteristics of these cases can be found easily. Recall that the effects of birefringence are determined by rotation of the input polarization about the axis on the sphere containing the eigenstates. For either the linear or elliptical eigenstates in this scenario, the starting point of the rotation is one of the poles (for left or right circular input). A change in the orientation of the eigenstates corresponds to traversal around the latitude containing those eigenstates. Now because the starting point of rotation is a pole, the ending point will always stop on the same latitude. This means the ellipticity of the output polarization will be the same for any orientation of eigenstates.

The circular analyzer has no preferred orientation in terms of coordinate systems. Therefore, any number of polarizations with the same ellipticity, regardless of

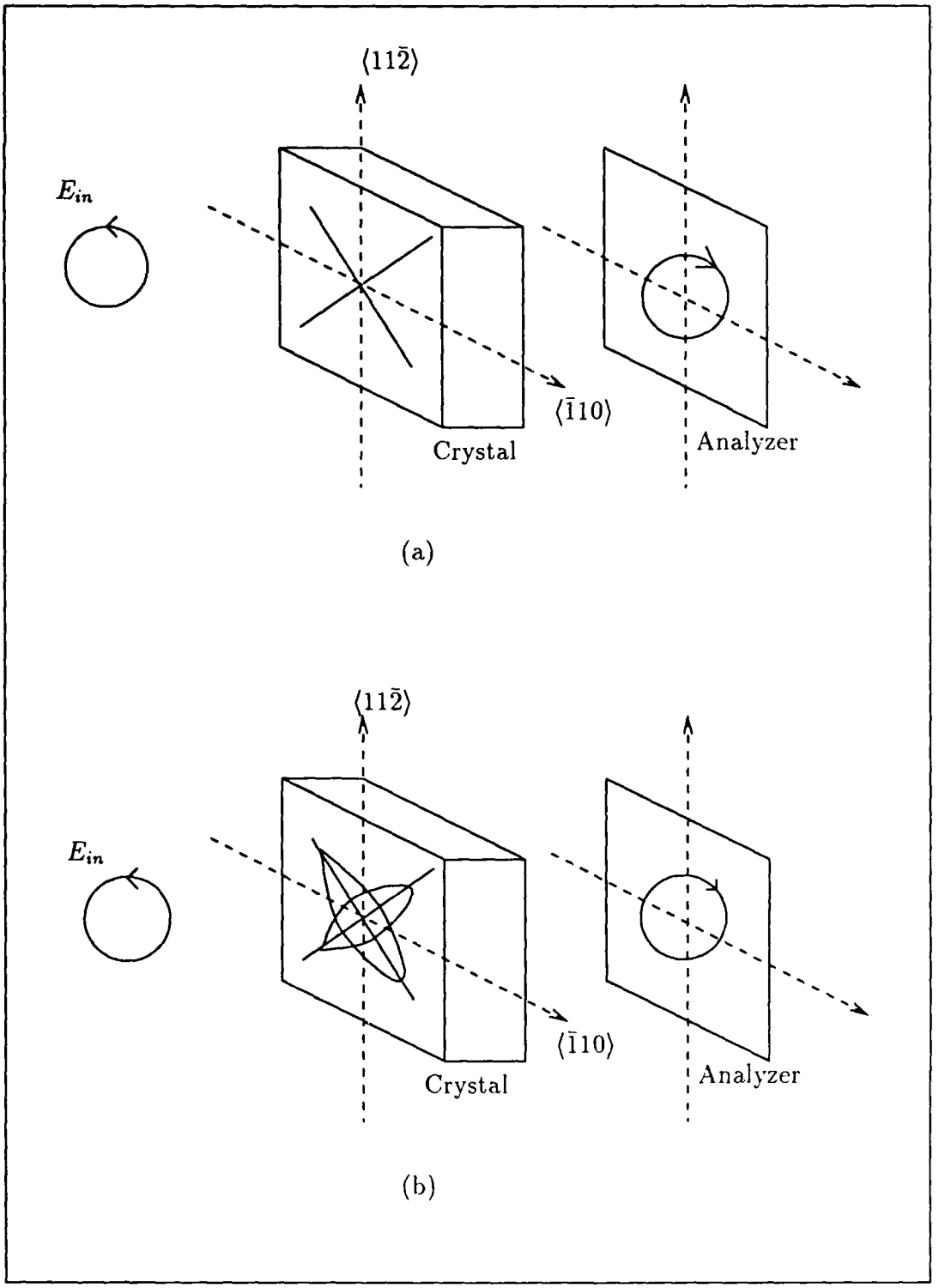

Figure 12. Circular input for (a) linear eigenstates and (b) elliptical eigenstates

orientation, incident on the analyzer should give the same value of output intensity. A constant output over all values of α is then expected for circularly polarized input.

Figure 13 shows that indeed the output intensity is constant for all α. This particular case involves $\xi = \pi$ and $\rho = \pi/9$. The curve for linear birefringence

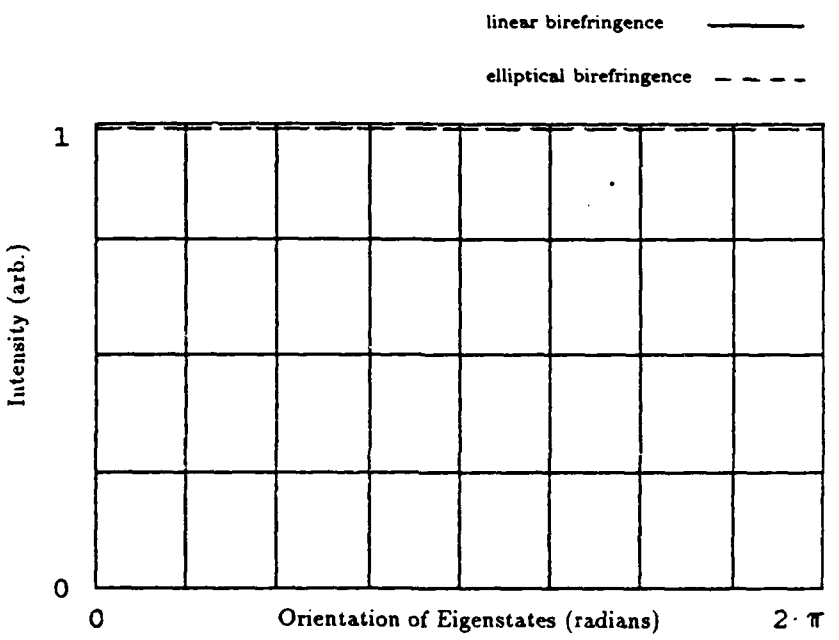

Figure 13. Intensity profile for circular input with $\xi = \pi$ and $\rho = \pi/9$

goes to unity because a half wave plate reverses the handedness of circular polarization, allowing it to match the circular analyzer. The results of Figures 31–37 in Appendix E show how that maximum intensity decreases with decreasing linear birefringence, and larger values of optical activity cause a more pronounced separation of the two curves.

The results of the circular input polarization with circular analyzer suggest great promise for imaging applications using the PRIZ. The problem of directional filtering is solved. Also, good contrast quality is possible, because for no transverse

field the input polarization will be extinguished by the analyzer, and the intensity level continuously increases as ξ increases.

Elliptical Input Polarization The final input polarization to investigate is elliptical. Again the system configuration is similar to Figure 9, where the polarizer and analyzer are now elliptical and orthogonal. The first eigenstate of Eq(34) will be the form used for the input, which will always have the major axis oriented in the x_1' direction. The Jones matrix system is

$$\begin{bmatrix} E'_{x_1} \\ E'_{x_2} \end{bmatrix} = \begin{bmatrix} dd^* & -cd^* \\ -c^*d & cc^* \end{bmatrix} \begin{bmatrix} \cos\alpha & \sin\alpha \\ -\sin\alpha & \cos\alpha \end{bmatrix} M \begin{bmatrix} \cos\alpha & -\sin\alpha \\ \sin\alpha & \cos\alpha \end{bmatrix} \begin{bmatrix} c \\ d \end{bmatrix} \quad (40)$$

where $c = i\rho$ and $d = (\Gamma - \xi)$, M is defined in the usual way.

The scenarios for the elliptical input polarization are shown in Figures 14(a) and 14(b). The analyzers here are orthogonal to the input polarization by having opposite handedness and interchanged major and minor axis directions.

The linear birefringence case of Figure 14(a) indicates that for any orientation of the linear eigenstates, the elliptical input will never match those states completely, so no extinction of the output can occur.

For the elliptical birefringence case of Figure 14(b), at successive 90° orientations of the eigenstates the input *ellipticity* will match that of the eigenstates, but the *handedness* will be the same only for successive 180° orientations. This suggests that the output will be totally extinguished only at these 180° intervals, while at the alternate 90° intervals the output will not be totally extinguished.

Figure 15 shows results for the case of $\xi = \pi$ and $\rho = \pi/9$. It is seen that the linear birefringence output is never fully extinguished, while the situation described above is evident for the elliptical birefringence results. The maximum intensity is seen to be at orientations of $\alpha = \pi/4$.

Figures 38–44 in Appendix F show results for the other values of ξ and ρ. Again, as the value of the linear birefringence decreases, the maximum intensity

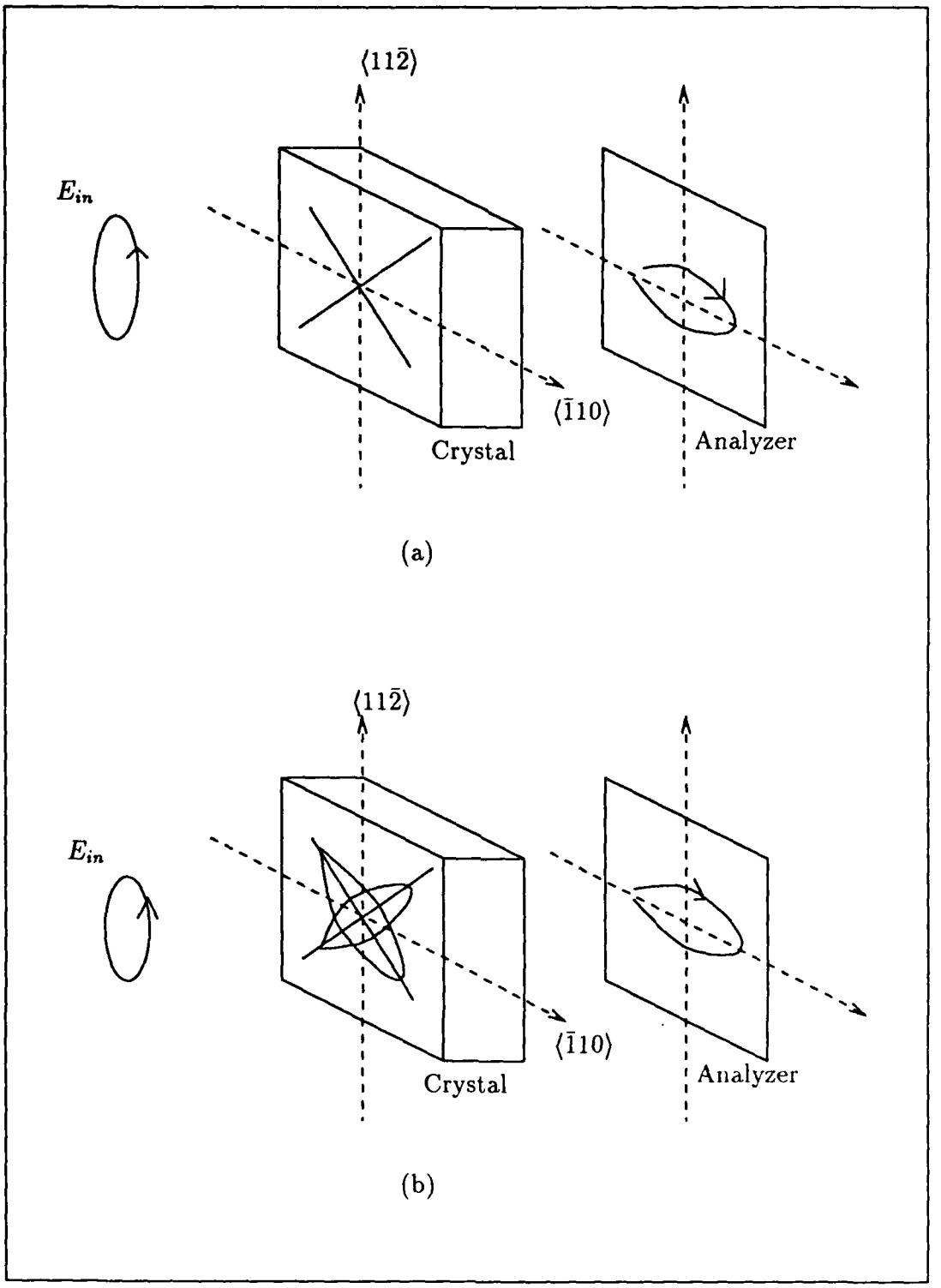

Figure 14. Elliptical input for (a) linear birefringence and (b) elliptical birefringence

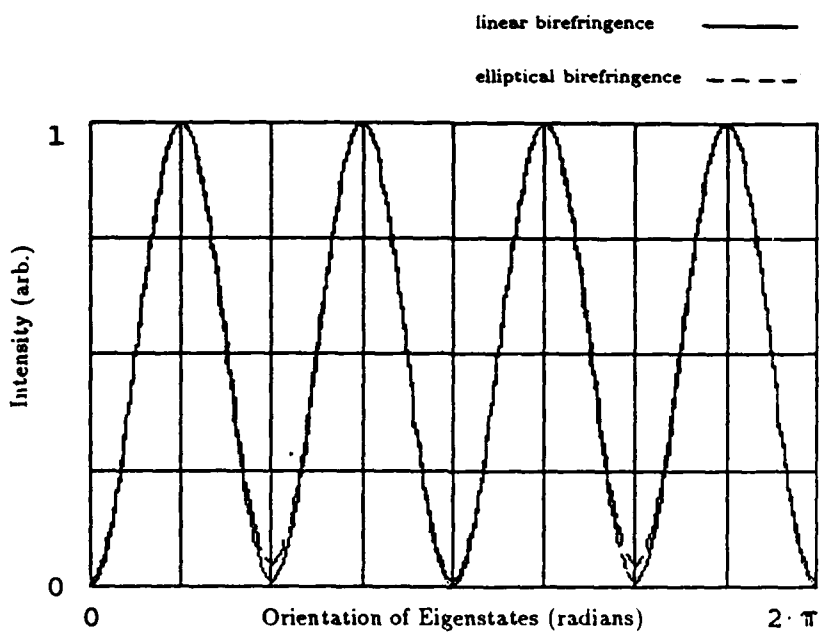

Figure 15. *Intensity* profile for elliptical input with $\xi = \pi$ and $\rho = \pi/9$

decreases. Also, as the amount of optical activity is increased, the separation of the curves for linear and elliptical birefringence become more pronounced.

The cases depicted by the elliptical input polarization do not have merit as far as imaging applications. Results show that not only is the output intensity directionally dependent and asymmetric, but also the system is impractical in that the polarizer and analyzer change forms for differing values of ξ and ρ.

Results for Variable Linear Birefringence

Images from a scene incident on the PRIZ typically contain areas of different incident photon energies; they also induce different directions of the transverse field in the device. The amount of incident energy is directly related to the induced linear birefringence (see Eq(33)). It is of interest then to determine the effects that variable linear birefringence has on the output intensity of linearly and elliptically

birefringent crystals.

The results of the previous section indicated that circular input polarization with an orthogonal circular analyzer did away with the directional filtering problem of the PRIZ imaging device. For this reason, circular input polarization will be the only polarization investigated in this section. The orientation of the eigenstates is no longer a factor, so the matrix system used for the analysis is

$$\begin{bmatrix} E'_{x1} \\ E'_{x2} \end{bmatrix} = \begin{bmatrix} bb^* & -ab^* \\ -a^*b & aa^* \end{bmatrix} \mathrm{M} \begin{bmatrix} a \\ b \end{bmatrix} \tag{41}$$

where $a = \cos(\pi/4)$, $b = i\sin(\pi/4)$, and M is Eq(19) or Eq(21). The variable for the M matrices will be ξ, which will range from 0 to π (the half wave point), and the amount of optical activity will be $\rho = \pi/9$.

The results of this case are shown in Figure 16. It turns out that the curve for linear birefringence follows a $\sin^2\xi$ pattern, while the curve for elliptical birefringence varies only slightly from this. The reason for only the slight variation is the relatively small value of optical activity.

The ideal situation, in terms of interfacing the PRIZ output intensity with a display gray scale, would have resulted in the output curves being linear. However, the results shown here characterize this output well, and can be used in future display design considerations.

Experimental Relevance

In experiments involving BSO at AFIT and elsewhere, the effects of optical activity have always been compensated for by simply setting the linear analyzer with a bias so that with no voltage applied, the rotated linear light would be extinguished. For example, in the AFIT PRIZ configuration, the analyzer was offset by approximately 10° (3:11). The experimental results using this configuration exhibited the asymmetry of output intensity similar to the elliptical input cases previously shown.

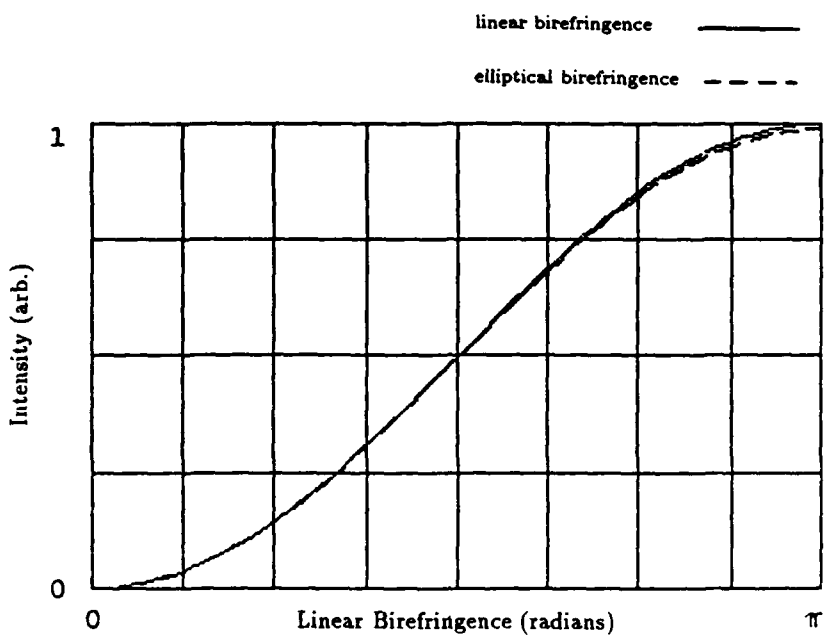

Figure 16. Output intensity as a function of linear birefringence with $\rho = \pi/9$

The system was modeled and test cases run to determine if any insights to this problem could be gained. The results for the case of a linear input polarization with $\xi = 2\pi/3$, $\rho = \pi/4.5$, and the crossed linear analyzer rotated an extra $\pi/9$, are given in Figure 17. These results show much similarity with the previous linear input cases discussed, and the problem of asymmetry is not apparent. In fact, all the cases run for this system configuration exhibited the same trends as the previous linear input cases, except for output shifted by the amount of the bias, and no asymmetric output was found.

In the article by Owechko and Tanguay (9:650–651), it was mentioned that a nonzero extinction of the analyzer causes the output intensity for linear input to become asymmetric. From the results just given, this is not the case. The AFIT lab configuration was investigated, and it was found that the input polarization for the read beam was not quite linear light. This problem was modeled by making the

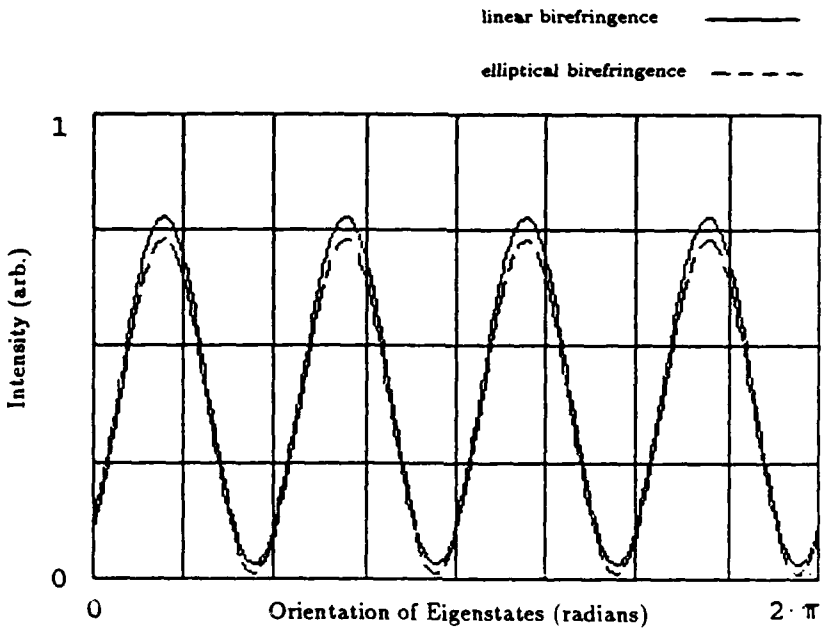

Figure 17. Output intensity for biased linear analyzer with $\xi = 2\pi/3$ and $\rho = \pi/4.5$

input polarization $\vec{E}$ elliptical:

$$\vec{E} = \begin{bmatrix} \cos\beta \\ i\sin\beta \end{bmatrix} \tag{42}$$

where $\beta = \pi/36$, providing a very small ellipticity. The results for a representative case of $\xi = 2\pi/3$ and $\rho = \pi/9$ are shown in Figure 18. The results, which are similar in form for other combinations of ξ and ρ, show clearly the asymmetric output intensity for *both* elliptical and linear birefringence cases.

Because circular polarization was shown to be best for imaging applications, the case of not quite circular polarization (analogous to the slightly elliptical case above) was also investigated, with $\beta = \pi/4.245$ in Eq(42). The system used a circular analyzer.

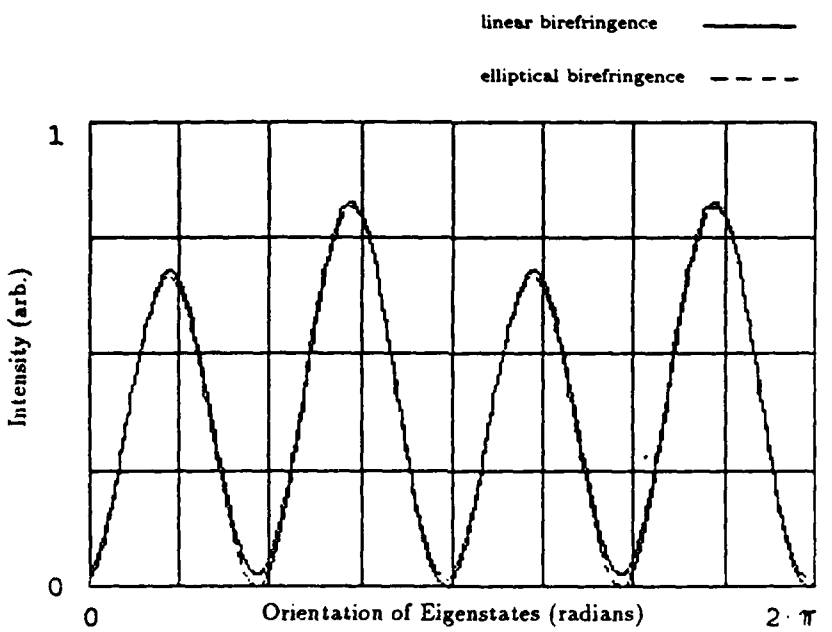

Figure 18. Elliptical input with linear analyzer; $\xi = 2\pi/3$ and $\rho = \pi/9$

The results in Figure 19 show that an asymmetry still occurs, but the maximum to minimum modulation of output intensity is less than for the analogous linear case. This reinforces the suggestion of using circular input polarization.

The final area looked at involved predicting the orientation of the crystal based on the direction of the asymmetry of output intensity as shown in Figure 18. The results of Figure 18 were obtained for the crystal orientation shown in Figure 22, where the input polarization was aligned with the $\langle 11\bar{2} \rangle$ direction.

Using the relation between the eigenstate direction and transverse field direction (Eq(32)), the simulation results agree with Capt Gardner's test results (3) in that the extinction occurs along the $\langle 11\bar{2} \rangle$ direction, and the higher intensity of the asymmetry occurs in the negative $\langle \bar{1}10 \rangle$ direction.

The crystal orientation was rotated 90° about the $\langle 111 \rangle$ axis for simulation (Figure 20). The results shown in Figure 21 are still consistent with the discussion

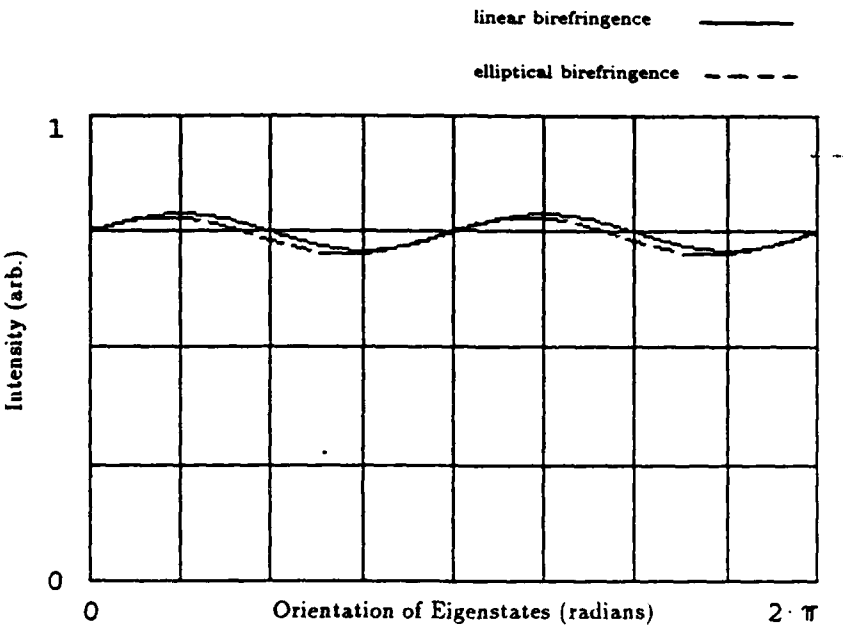

Figure 19. Elliptical input with circular analyzer; $\xi = 2\pi/3$ and $\rho = \pi/9$

above; i.e. the extinction is along the $\langle 11\bar{2} \rangle$ direction, and the higher intensity of the asymmetry is in the negative $\langle \bar{1}10 \rangle$ direction. Therefore, the asymmetry direction is predictable if the crystal orientation is known.

Summary

This chapter presented a discussion of the Jones matrix configuration used for computations, the concept of polarizer-analyzer pairs, variables and parameters used in the computations, and results of these computations. The first set of trials consisted of linear, circular, and elliptical input polarizations with respective orthogonal analyzers. Comparisons of linear and elliptical birefringence among these cases showed that, especially for smaller values of ξ (representing linear birefringence) approaching the optical activity ρ, the intensity outputs of the elliptically birefringent crystal were noticeably different from the corresponding linearly birefringent crystal.

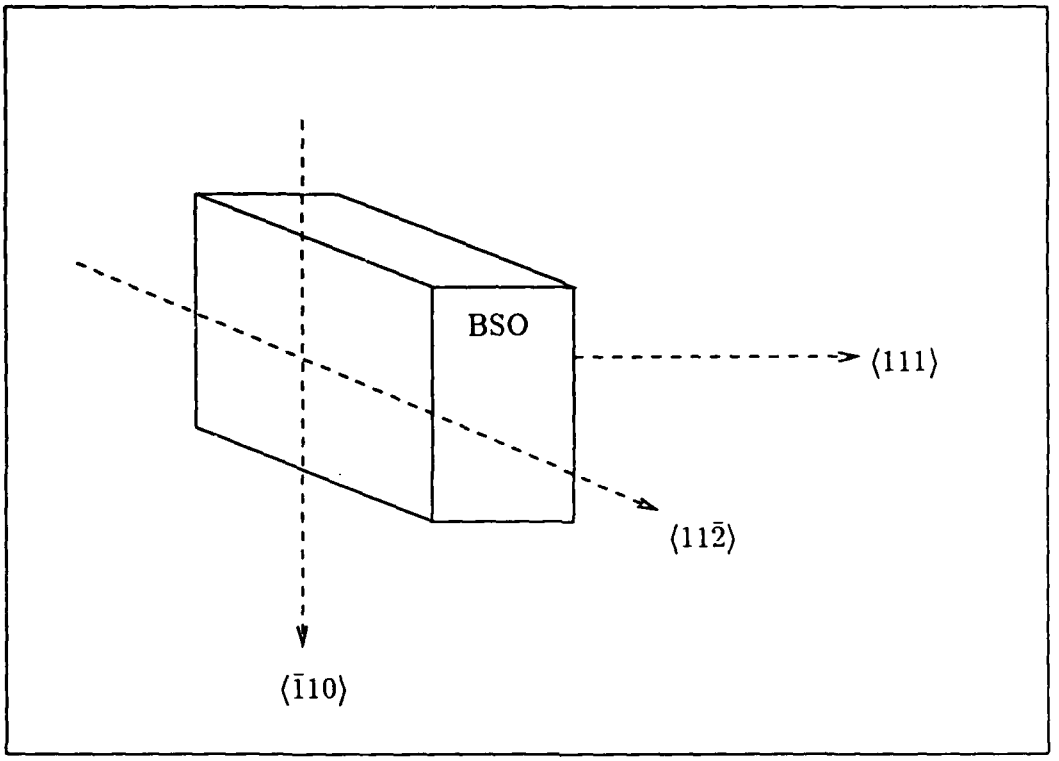

Figure 20. Crystal orientation for asymmetry test

As far as imaging quality characteristics, the circular input polarization case gave results which were most promising in relation to contrast and symmetry of the output, since no directional filtering was evident with this case. The response of variable linear birefringence was determined to follow a sine squared pattern, which is of concern for displaying the output imagery. Finally, actual experimental results were used to show that asymmetric output intensity direction can be determined by the crystal orientation of the PRIZ device.

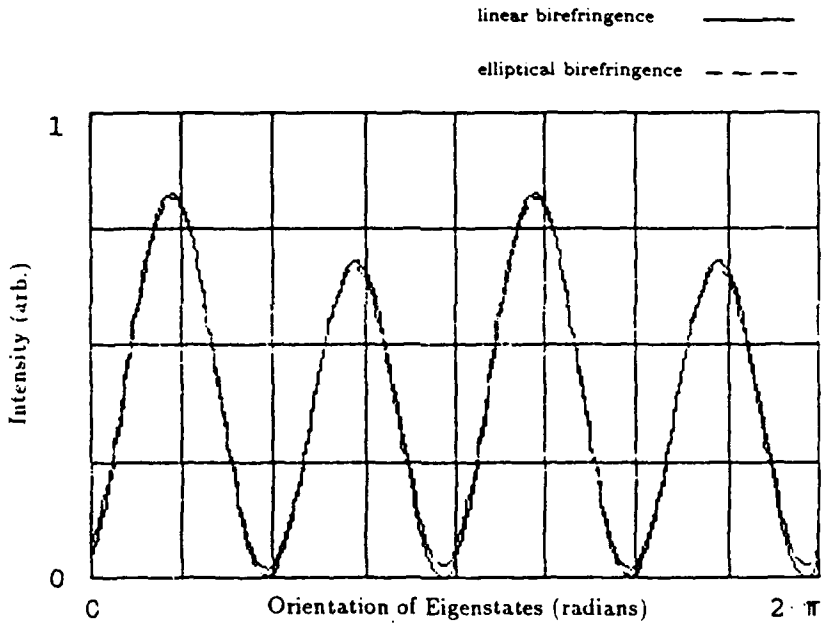

Figure 21. Elliptical input with linear analyzer for crystal as oriented in Figure 20

IV. Conclusions and Recommendations

A description of an elliptically birefringent crystal was developed using two separate but consistent mathematical forms: the Poincaré sphere and Jones matrices. These methods were used to show that the crystal is represented by elliptical birefringence, or elliptically polarized eigenstates. Furthermore, the elliptical birefringence was shown to be a nonlinear combination of the linear birefringence and the circular birefringence (optical activity).

The results of a mathematical representation led to an investigation of an imaging device known as the PRIZ, which uses the photorefractive, optically active crystal BSO. A series of computations using Jones matrices was done to compare performance of a device where optical activity is factored in with a device where optical activity is ignored. Variables and parameters used in these computations included type of input polarization, values of linear birefringence and optical activity, and the orientation of the eigenstates of the crystal with respect to the direction of the transverse internal electric field.

Results of analysis showed that for values of the linear birefringence close to that of the optical activity, the intensity curves for elliptical birefringence made a noticeable change from the linear birefringence curves. Also, the directional filtering problem for linear polarization already mentioned in the literature was shown to be present for elliptical polarization as well. Circular input with an orthogonal circular analyzer, however, showed no such filtering. Since imaging quality is directly affected by this filtering, it is recommended that circular input polarization with an orthogonal circular analyzer be used in future applications of this device.

Other results related to the experimental procedure showed that an asymmetry of output intensity developed for even slightly elliptically polarized input. This asymmetry was not present for perfectly linear input, which leads to the conclusion

that — should directional filtering be acceptable but the asymmetry not — great care should be taken to produce polarization as linear as possible. By the same token, slightly non-circular input polarization also causes an asymmetry (though not as pronounced as the linear case), so circular input applications should have polarization as circular as possible.

Perhaps the most pertinent aspect of these results is it appears that, for the application of BSO as used in the AFIT PRIZ device, optical activity can probably be ignored without much deviation from results obtained with including it. This does not necessarily mean that for different materials or other applications this should be the case. This thesis has laid the groundwork for future investigations involving elliptically birefringent materials, which can now be carried out with greater ease.

Appendix A. *PRIZ Spatial Light Modulator*

The PRIZ device uses photorefractive BSO with the electric field of the linear electro-optic effect applied in the longitudinal direction (11:816). For this application, this direction is the direction of propagation of the incident light $\vec{E}$ (Figure 22). The crystallographic axes are chosen from crystal symmetry to be the $\langle 111 \rangle$ cut. If

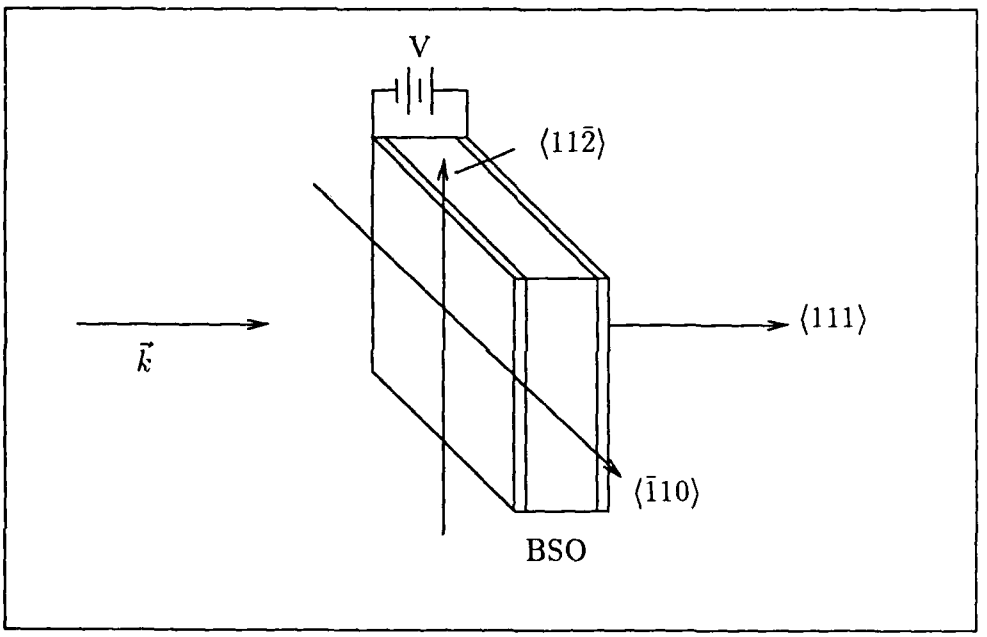

Figure 22. Crystal orientation of $\langle 111 \rangle$ PRIZ device, with applied field parallel to direction of propagation

this is considered the z direction of a right-hand coordinate system, then the x and y directions are $\langle 11\bar{2} \rangle$ and $\langle \bar{1}10 \rangle$, respectively. The material is cut so that the $\langle 111 \rangle$ surfaces are plane parallel.

The basic operation of the PRIZ is depicted in Figure 23 (3:12). An image can be written onto the BSO crystal (3) by means of the photorefractive effect, which alters the indices of refraction at locations where the object (2) illumination falls.

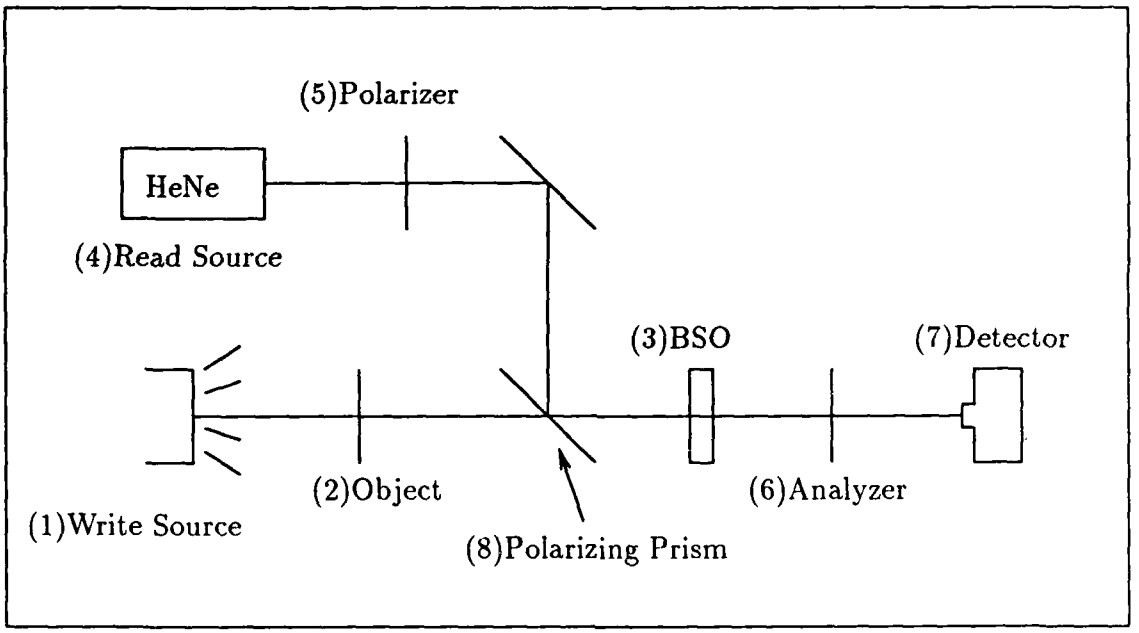

Figure 23. PRIZ imaging configuration

This stored information is retrieved using a linearly polarized read beam (4), which is modified locally by the induced birefringence in the crystal. An analyzer (6) crossed with respect to the polarizer (5) will then give the intensity variation of the image via amplitude modulation. This image can be detected (7) by a television camera or other such device as suited to the application (9:636).

Appendix B. *Electromagnetic Description of Elliptical Birefringence*

The material equation, which describes the effect of the electromagnetic field on the material, is given by

$$\vec{D} = \epsilon \vec{E} \tag{43}$$

where $\vec{D}$ is the electric displacement vector describing the induced polarization, $\vec{E}$ is the electric field vector, and ϵ is the dielectric tensor which relates the two. The dielectric tensor is unique to each material and the form is dependent on crystal symmetry. For example, the crystal point group 23, of which BSO is a member, has the dielectric tensor

$$\epsilon = \begin{bmatrix} \epsilon_{11} & 0 & 0 \\ 0 & \epsilon_{11} & 0 \\ 0 & 0 & \epsilon_{11} \end{bmatrix} \tag{44}$$

This is the form for the crystal oriented in the principal coordinate system, i.e. $\vec{D}$ is parallel to $\vec{E}$ along these axes.

For much work in crystal optics, it is assumed that ϵ is a constant independent of other influences on the crystal. With optical activity, however, ϵ is dependent on the direction of propagation $\vec{k}$. The form of the dielectric tensor in this case becomes

$$\epsilon_{ij}(\vec{k}) = \epsilon_{ij} + \epsilon_0 \sum_l g_{ijl} K_l \tag{45}$$

where ϵ_{ij} are the tensor components without optical activity, ϵ_0 is the permittivity of free space, K_l are the components of the specific direction of propagation $\vec{K}$, and g_{ijl} are third order tensor components which represent optical activity (7:120-121). Summation over repeated indices shall be assumed unless otherwise stated.

If a medium doesn't attenuate transmitted waves, then the symmetry of ϵ_{ij} is

$$\epsilon_{ij} = \epsilon_{ji}^* \tag{46}$$

where ϵ_{ji}^* is the complex conjugate of ϵ_{ji}. This means that ϵ_{ij} is Hermitian if the field energy is conserved. If the energy is invariant under time reversal, then

$$\epsilon_{ij}(-\vec{k}) = \epsilon_{ji}(\vec{k}) \tag{47}$$

Optical activity does not contribute to the electric energy density, so the conditions of Eqs(46) and (47) apply to Eq(45). This leads to the symmetry of

$$\begin{aligned} g_{ijl} &= g_{jil}^* \\ g_{ijl} &= -g_{jil} \end{aligned} \tag{48}$$

Therefore, it is strictly an imaginary tensor which is antisymmetric in the first two indices. Since g_{ijl} is purely imaginary, it can be represented by

$$\begin{aligned} g_{ijl} &= i\gamma_{ijl} \\ \gamma_{ijl} &= -\gamma_{jil} \end{aligned} \tag{49}$$

where γ_{ijl} is a polar third rank tensor. (Tensors can be described as either *polar* or *axial*. A polar tensor transforms like a product of coordinates for both rotations and rotation-inversions, whereas an axial tensor transforms like a product of coordinates under rotations, but like (-1) times the product of coordinates under rotation-inversions (7:22). See Appendix C for a related discussion.)

Because of the antisymmetry associated with γ_{ijl}, the optical activity term can be represented by a second rank tensor g_{ml}, known as the *gyration tensor*:

$$\gamma_{ijl} = \sum_m \epsilon_{ijm} g_{ml} \tag{50}$$

where ϵ_{ijm} is the antisymmetric triple product, and m represents contracted indices such that $23 \rightarrow 1$, $31 \rightarrow 2$, and $12 \rightarrow 3$. The antisymmetric triple product is defined by

$$\epsilon_{ijm} = \begin{cases} 1 & \text{for } ijm = 123,312,231 \\ -1 & \text{for } ijm = 321,132,213 \\ 0 & \text{for all others} \end{cases} \tag{51}$$

The gyration tensor is an axial tensor because the inversion of the coordinate system would not necessarily change the signs of the components of the tensor (8:40). So under the inversion symmetry ($\bar{1}$), g_{ml} goes into its negative. This leads to the fact that any centrosymmetric crystal cannot exhibit optical activity. Appendix C describes the form of the gyration tensor for BSO, and how it was derived using crystal symmetry.

A vector $\vec{G}$, known as the *gyration vector*, can now be defined such that it has components

$$G_m = \sum_l g_{ml} K_l \tag{52}$$

Now the dielectric tensor of Eq(45) can be represented by

$$\epsilon_{ij}(\vec{k}) = \epsilon_{ij} + i\epsilon_0 \sum_m \epsilon_{ijm} G_m \tag{53}$$

The material equation, which has the form

$$D_i = \sum_j \epsilon_{ij}(\vec{k}) E_j \tag{54}$$

can now be expressed as

$$D_i = \sum_j \epsilon_{ij} E_j + i\epsilon_0 (\vec{E} \times \vec{G})_i \tag{55}$$

Equating this expression containing optical activity with the relation between $\vec{D}$ and $\vec{E}$ from Maxwell's equations,

$$D_i = n^2(\epsilon_0 E_i - \epsilon_0 K_i(\vec{K} \cdot \vec{E})) \tag{56}$$

will lead to a solution for the two independent indices of refraction n^I and n^{II} which are the eigenvalues of the eigenstates of the crystal. If it is assumed that the crystal is oriented in the principal coordinate system, then the dielectric tensor ϵ will have only three diagonal terms, represented by ϵ_i. It is assumed that the magnitude of $\vec{G}$ is much less than ϵ_i, so that solutions involving $\vec{G}$ can be thought of as perturbations

of solutions for which $\vec{G} = 0$. For the case of $\vec{G} = 0$, the two independent indices are represented by n' and n''. Using Eqs(55) and (56) to eliminate D_i gives

$$E_i(\epsilon_i - \epsilon_0 n^2) + \epsilon_0 n^2(\vec{E} \cdot \vec{K})K_i - i\epsilon_0(\vec{G} \times \vec{E})_i = 0 \tag{57}$$

The secular determinant of the homogeneous equations of Eq(57) is given by

$$\epsilon_0^2 \left(\sum_i \epsilon_i K_i^2\right) n^4 - \epsilon_0 \left(\sum_{i,j>i} \epsilon_i \epsilon_j \left(K_i^2 + K_j^2\right) - \epsilon_0^2 |\vec{K} \times \vec{G}|^2\right) n^2 + (\epsilon_1 \epsilon_2 \epsilon_3 - \epsilon_0^2 \textstyle\sum_i \epsilon_i G_i^2) = 0 \tag{58}$$

By grouping the terms dependent on $\vec{G}$ on the right side of Eq(58), two characteristic solutions for n^2 can be determined from

$$(n^2 - n'^2)(n^2 - n''^2) = \frac{\sum_i \epsilon_i G_i^2 - \epsilon_0 n^2 |\vec{K} \times \vec{G}|^2}{\sum_i \epsilon_i K_i^2} \tag{59}$$

where in the absence of optical activity, the right side of Eq(59) goes to zero. For a cubic crystal, $\epsilon_0 n^2 = \epsilon_1 = \epsilon_2 = \epsilon_3$, so Eq(59) simplifies to

$$(n^2 - n'^2)(n^2 - n''^2) = (\vec{K} \cdot \vec{G})^2 \tag{60}$$

The term $(\vec{K} \cdot \vec{G})$ is a scalar which can be represented by g, where

$$g = \sum_{m,l} g_{ml} K_m K_l \tag{61}$$

Equation (60) is now written as

$$\left(n^2 - n'^2\right)\left(n^2 - n''^2\right) = g^2 \tag{62}$$

The positive solutions to Eq(62) are n^I and n^{II}, which are the eigenindices for the normal modes of propagation in the linearly birefringent, optically active crystal. (Remember that although BSO is a cubic crystal, a field applied induces a birefringence.) The phase difference Δ (per unit thickness) between these two normal modes is given by

$$\Delta = \frac{2\pi}{\lambda_o}\left(n^I - n^{II}\right) \tag{63}$$

where λ_o is the specific wavelength of the incident light. Now

$$\left(n^I - n^{II}\right)^2 = n^{I^2} + n^{II^2} - 2\left(n^{I^2} n^{II^2}\right)^{1/2} \tag{64}$$

Also, the roots of Eq(62) are n^{I^2} and n^{II^2}. So it follows that

$$\left(n^I - n^{II}\right)^2 = n'^2 + n''^2 - 2\left(n'^2 n''^2 - g^2\right)^{1/2} \tag{65}$$

Using Eq(65) and the assumption that $g \ll n'n''$, Eq(63) can be written

$$\Delta^2 = \frac{4\pi^2}{\lambda_o^2}\left[(n' - n'')^2 + \frac{g^2}{n'n''}\right] \tag{66}$$

If $\bar{n}$ is defined as a mean refractive index equal to $(n'n'')^{1/2}$, then Eq(66) becomes

$$\Delta^2 = \delta^2 + (2\rho)^2 \tag{67}$$

where δ is the linear birefringence, equal to $\frac{2\pi}{\lambda_o}(n' - n'')$, and ρ is the optical rotatory power, now defined as

$$\rho = \frac{\pi g}{\lambda_o \bar{n}} \tag{68}$$

Eq(68) can be found from setting $n' = n''$ in Eq(62), solving for the difference $n^I - n^{II}$, and then substituting that into Eq(1).

Appendix C. *Gyration Tensor for Crystal Point Group 23*

Consider a tensor in an unprimed coordinate system which undergoes a symmetry operation into a primed coordinate system. The respective tensor components for each coordinate system are still required to be equal. Following the arguments of Juretschke (7:24), a practical way to go about this is to consider only the generating elements of the symmetry group. If these generating elements contain values of ± 1 only, the transformation is simplified. For example, for the point group 23, the generating elements are 2 and B:

$$2 = \begin{bmatrix} -1 & 0 & 0 \\ 0 & -1 & 0 \\ 0 & 0 & 1 \end{bmatrix} \qquad B = \begin{bmatrix} 0 & 1 & 0 \\ 0 & 0 & 1 \\ 1 & 0 & 0 \end{bmatrix} \tag{69}$$

where 2 defines a twofold rotation about the z axis, and B defines a threefold rotation about a cube body diagonal (7:195). Taking the B element first, the transformation gives

$$\begin{aligned} \alpha_{11} &= \alpha_{22} \\ \alpha_{12} &= \alpha_{23} \\ \alpha_{13} &= \alpha_{21} \\ \alpha_{21} &= \alpha_{32} \\ \alpha_{22} &= \alpha_{33} \\ \alpha_{23} &= \alpha_{31} \\ \alpha_{31} &= \alpha_{12} \\ \alpha_{32} &= \alpha_{13} \\ \alpha_{33} &= \alpha_{11} \end{aligned} \tag{70}$$

So the relations from this element are

$$\alpha_{11} = \alpha_{22} = \alpha_{33}$$

$$\alpha_{12} = \alpha_{23} = \alpha_{31}$$
$$\alpha_{13} = \alpha_{21} = \alpha_{32} \tag{71}$$

Then in a like manner applying this tensor to the generating element 2 results in

$$\alpha_{11} = \alpha_{22} = \alpha_{33}$$
$$\alpha_{12} = \alpha_{23} = \alpha_{31} = -\alpha_{23} = -\alpha_{31} = 0$$
$$\alpha_{13} = \alpha_{21} = \alpha_{32} = -\alpha_{13} = -\alpha_{32} = 0 \tag{72}$$

The results of Eq(72) then lead to the general second order tensor

$$\alpha_{ij} = \begin{bmatrix} \alpha_{11} & 0 & 0 \\ 0 & \alpha_{11} & 0 \\ 0 & 0 & \alpha_{11} \end{bmatrix} \tag{73}$$

which is directly analogous to the gyration tensor so that for the 23 point group

$$g_{ml} = \begin{bmatrix} g_{11} & 0 & 0 \\ 0 & g_{11} & 0 \\ 0 & 0 & g_{11} \end{bmatrix} \tag{74}$$

Appendix D. *Output Intensity for Linear Input*

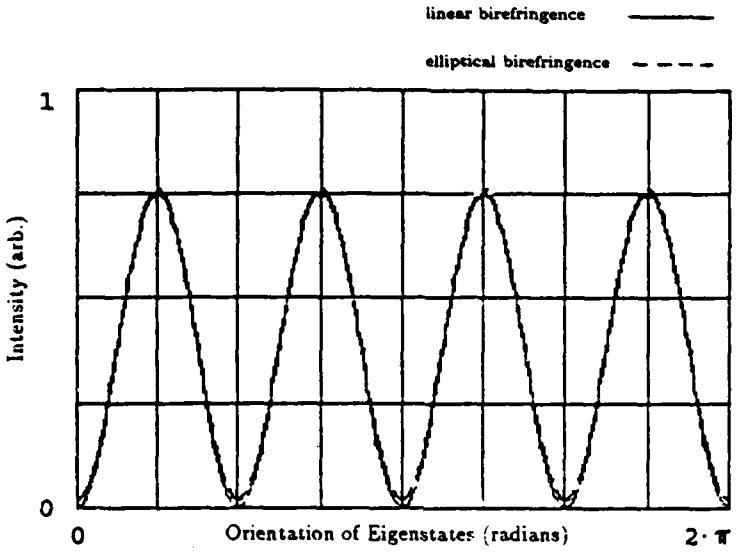

Figure 24. Intensity for $\xi = 2\pi/3$ and $\rho = \pi/9$

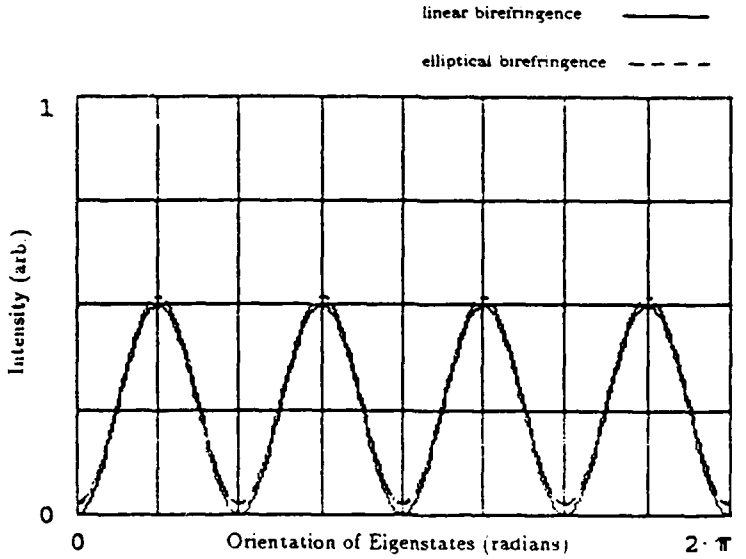

Figure 25. Intensity for $\xi = \pi/2$ and $\rho = \pi/9$

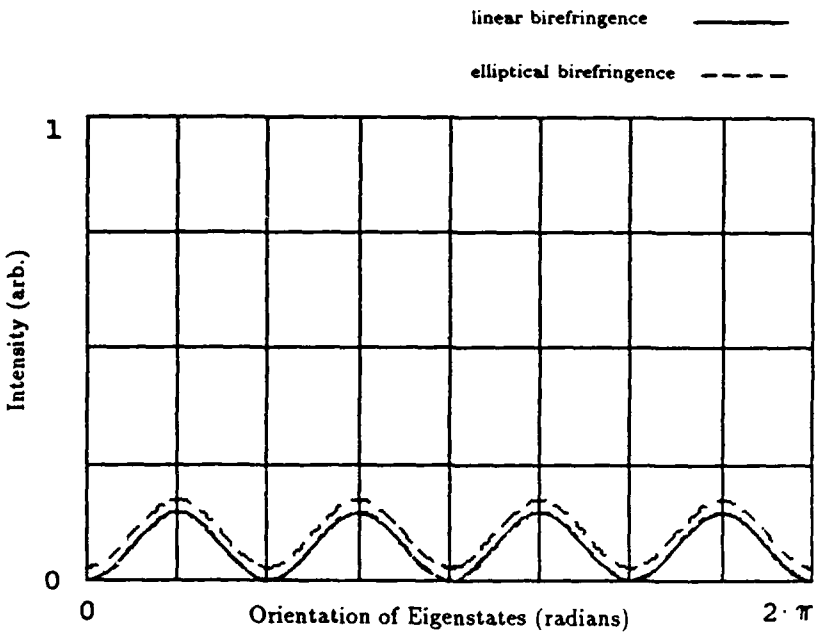

Figure 26. Intensity for $\xi = \pi/4$ and $\rho = \pi/9$

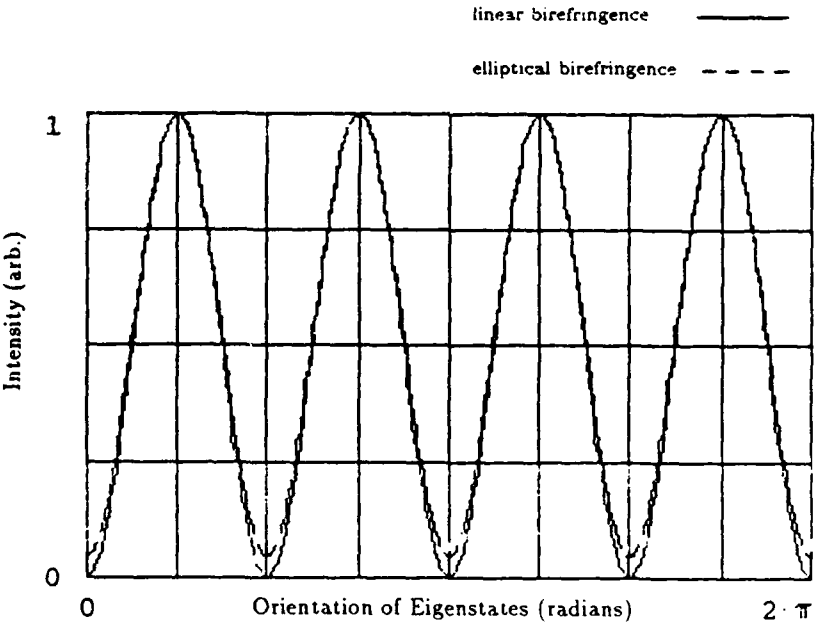

Figure 27. Intensity for $\xi = \pi$ and $\rho = \pi/4.5$

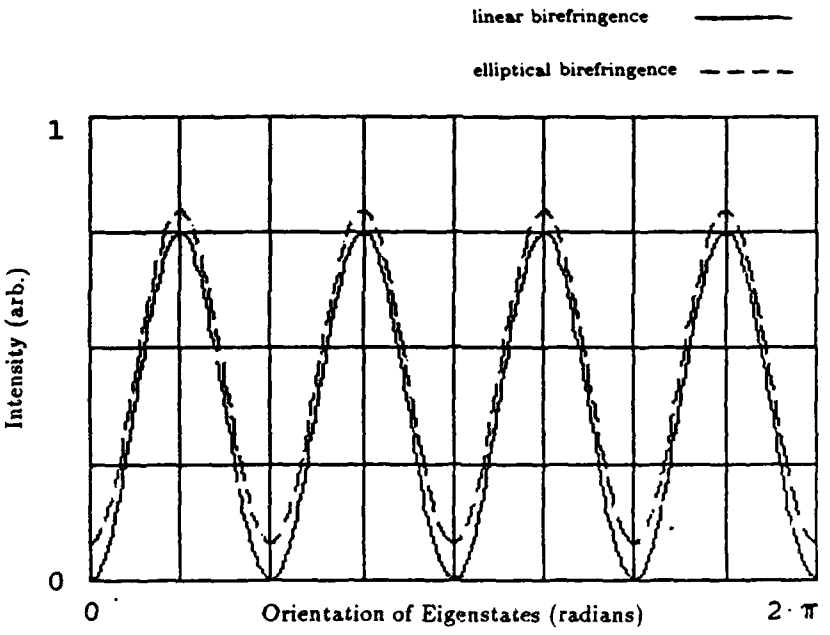

Figure 28. Intensity for $\xi = 2\pi/3$ and $\rho = \pi/4.5$

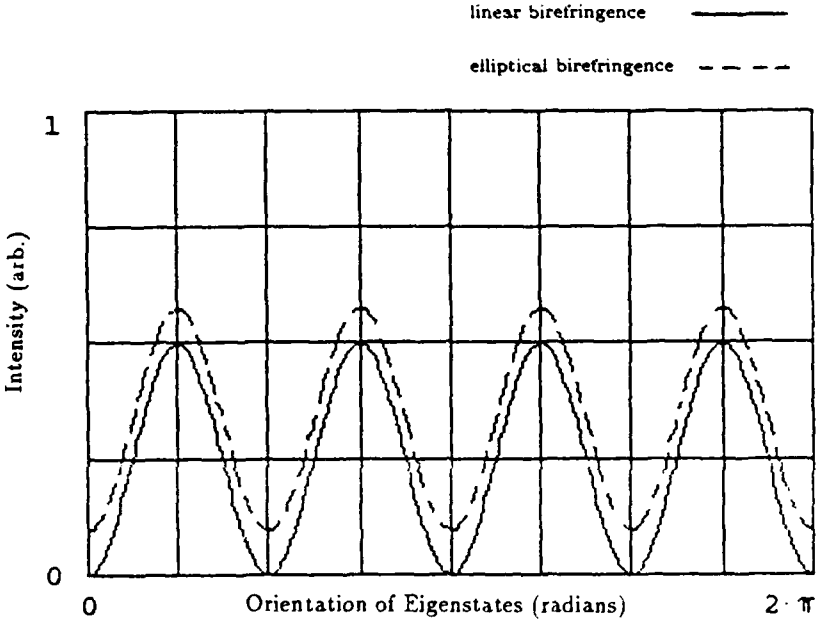

Figure 29. Intensity for $\xi = \pi/2$ and $\rho = \pi/4.5$

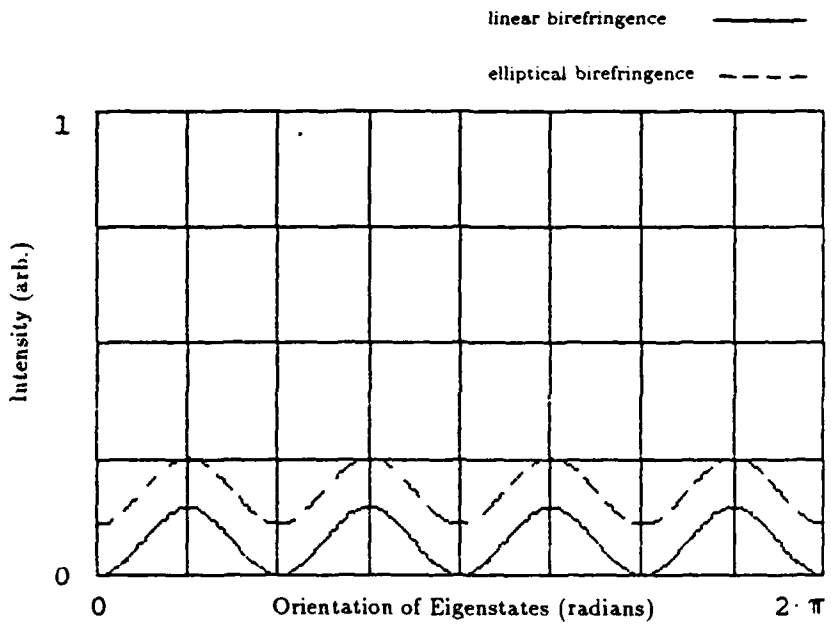

Figure 30. Intensity for $\xi = \pi/4$ and $\rho = \pi/4.5$

Appendix E. *Output Intensity for Circular Input*

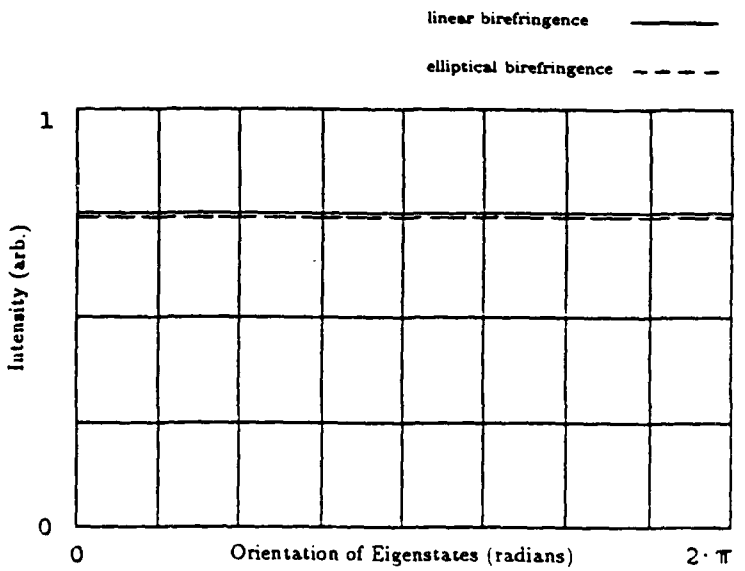

Figure 31. Intensity for $\xi = 2\pi/3$ and $\rho = \pi/9$

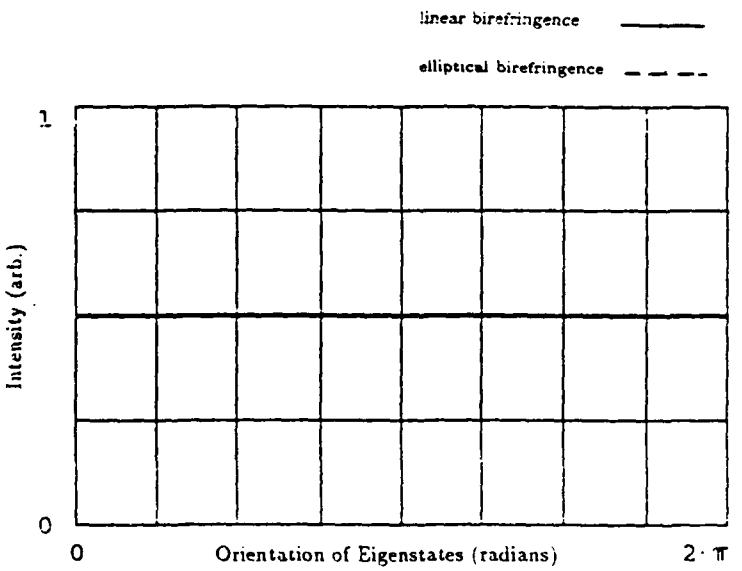

Figure 32. Intensity for $\xi = \pi/2$ and $\rho = \pi/9$

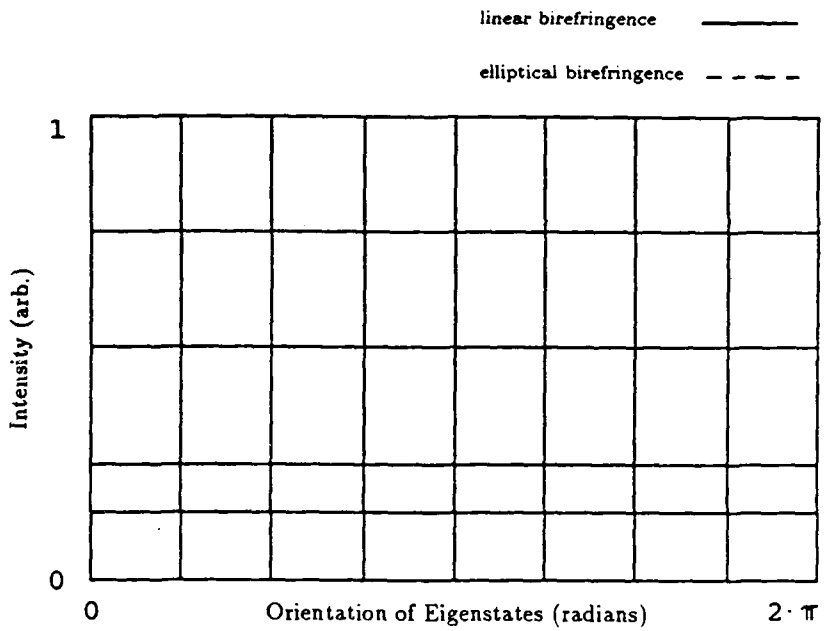

Figure 33. Intensity for $\xi = \pi/4$ and $\rho = \pi/9$

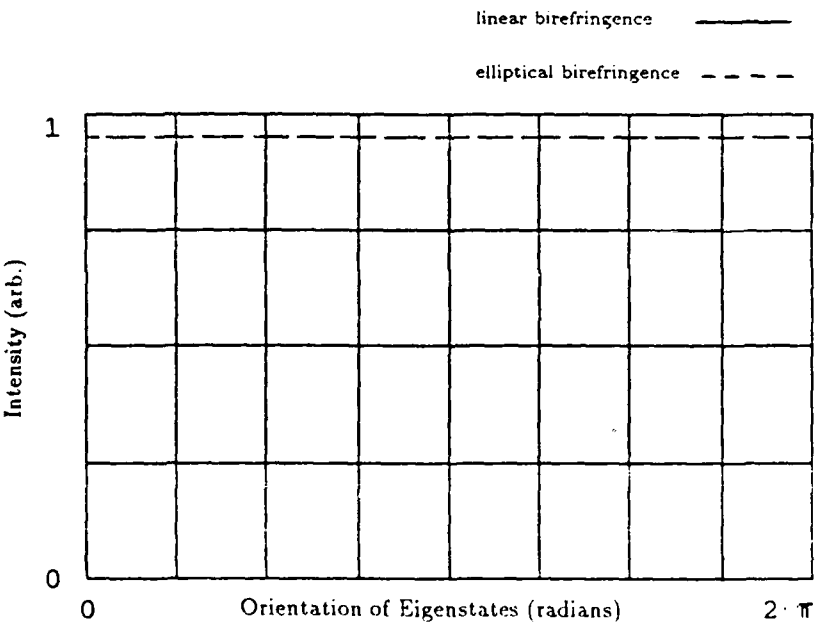

Figure 34. Intensity for $\xi = \pi$ and $\rho = \pi/4.5$

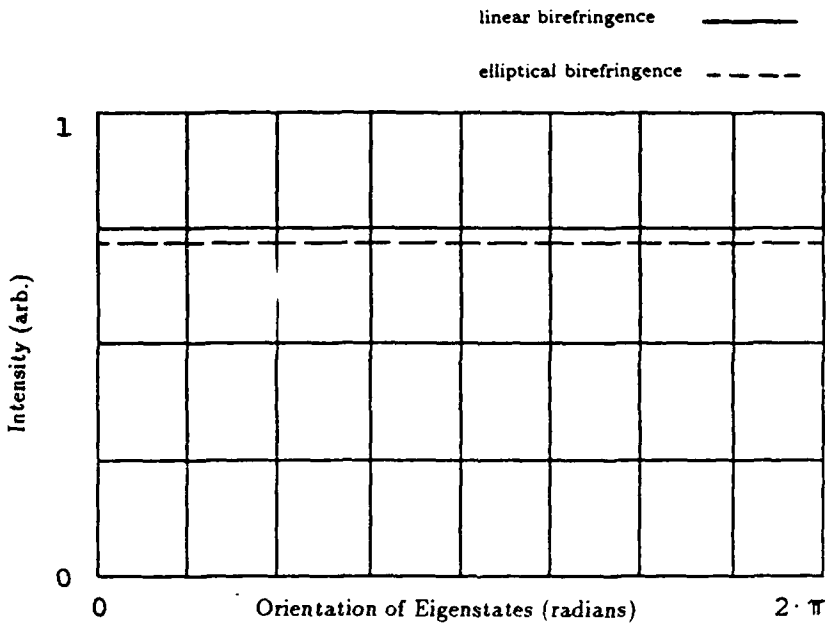

Figure 35. Intensity for $\xi = 2\pi/3$ and $\rho = \pi/4.5$

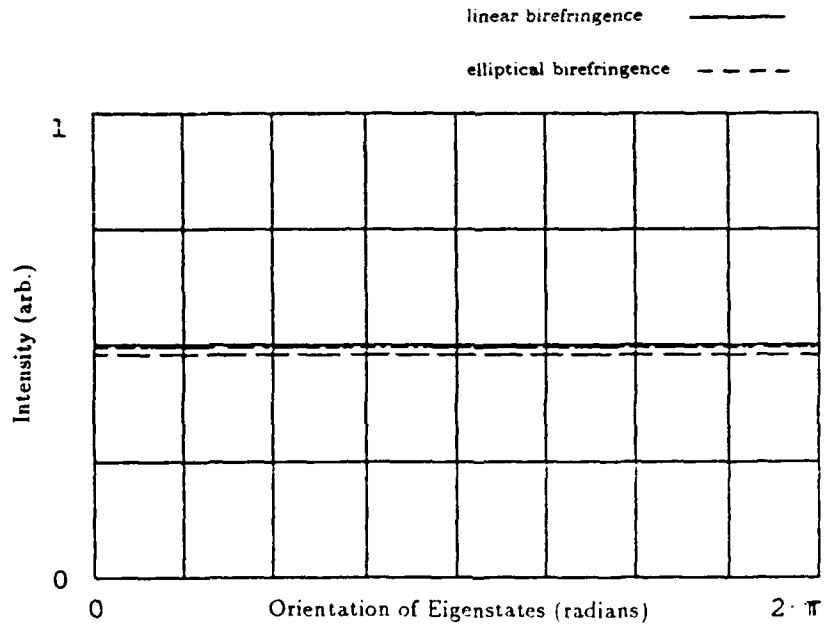

Figure 36. Intensity for $\xi = \pi/2$ and $\rho = \pi/4.5$

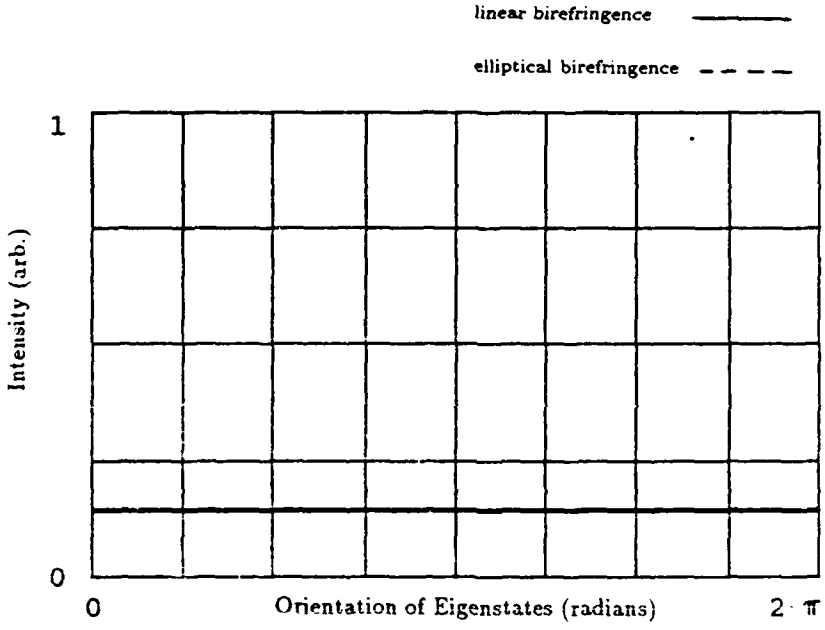

Figure 37. Intensity for $\xi = \pi/4$ and $\rho = \pi/4.5$

Appendix F. *Output Intensity for Elliptical Input*

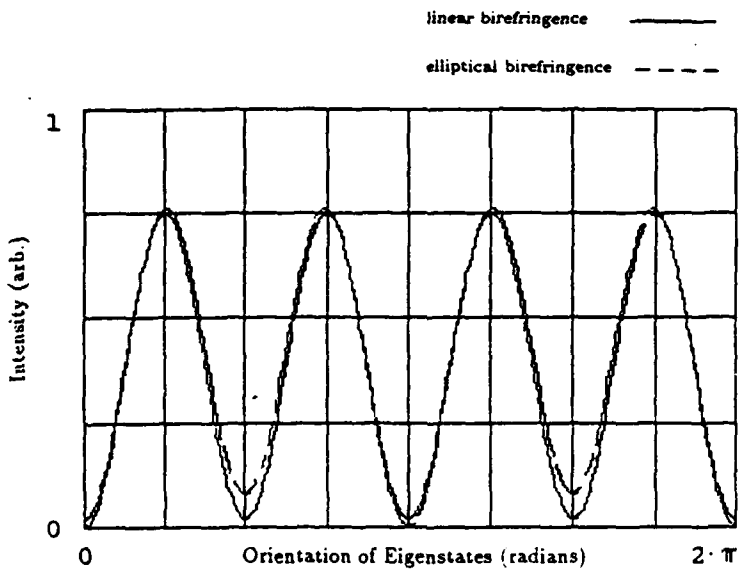

Figure 38. Intensity for $\xi = 2\pi/3$ and $\rho = \pi/9$

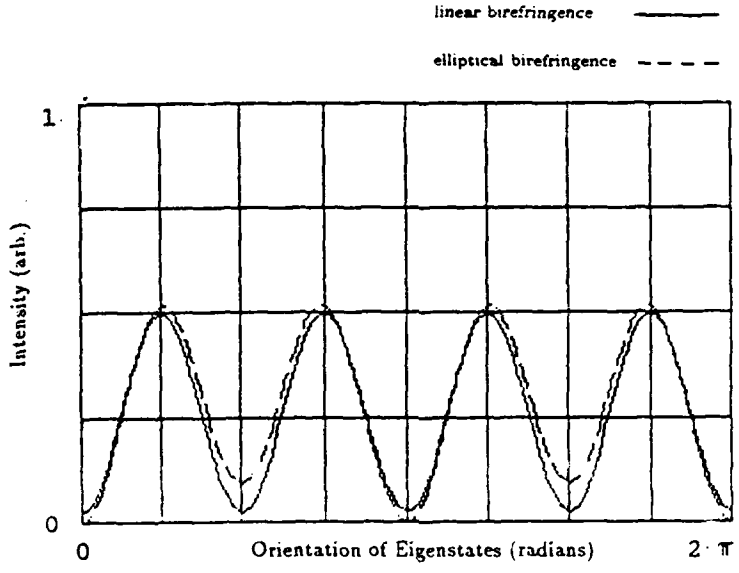

Figure 39. Intensity for $\xi = \pi/2$ and $\rho = \pi/9$

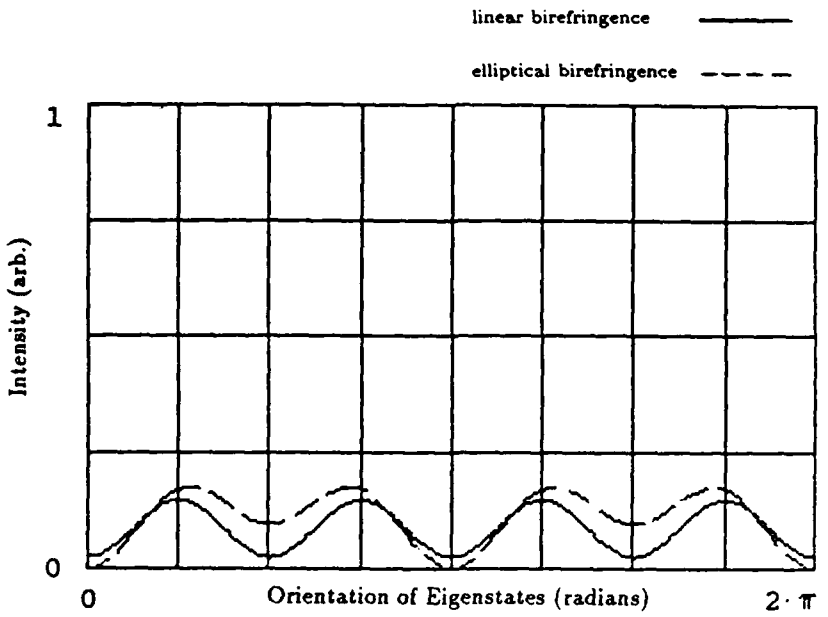

Figure 40. Intensity for $\xi = \pi/4$ and $\rho = \pi/9$

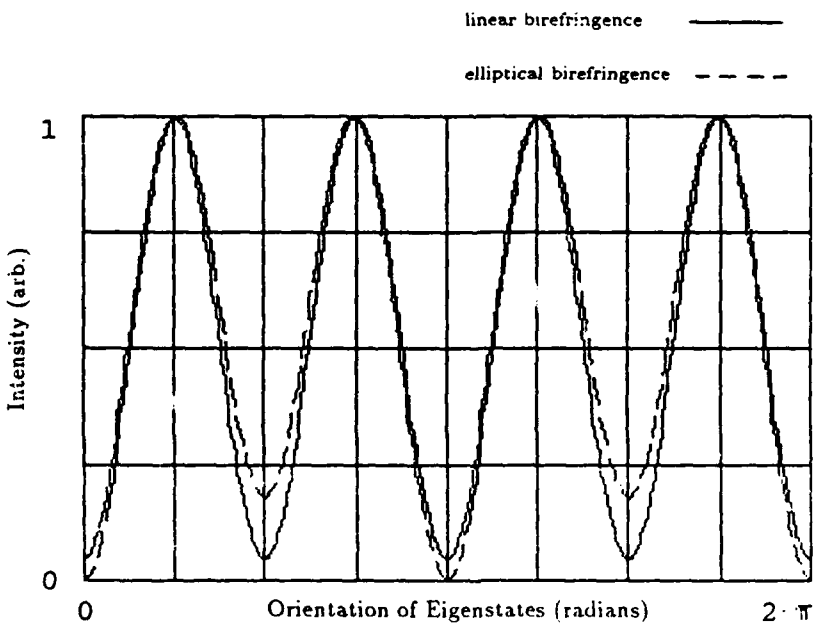

Figure 41. Intensity for $\xi = \pi$ and $\rho = \pi/4.5$

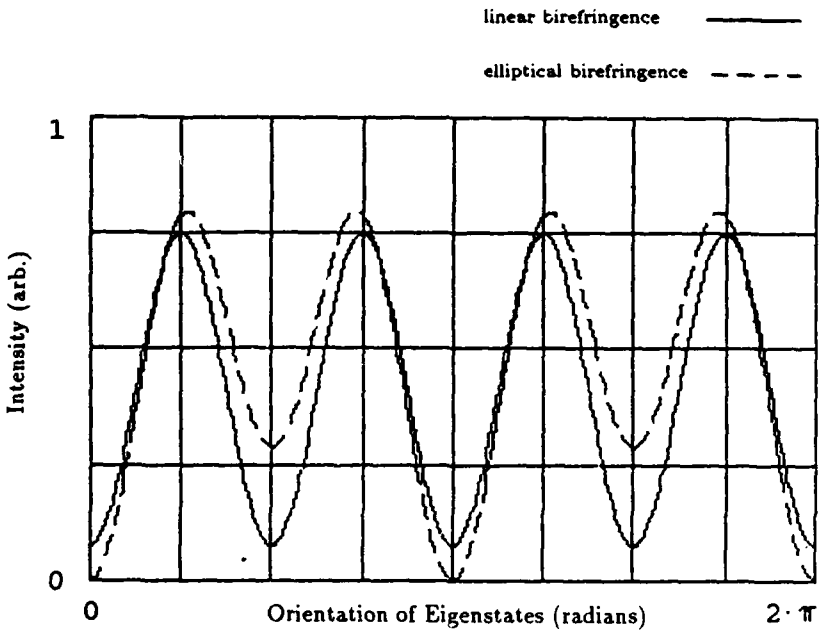

Figure 42. Intensity for $\xi = 2\pi/3$ and $\rho = \pi/4.5$

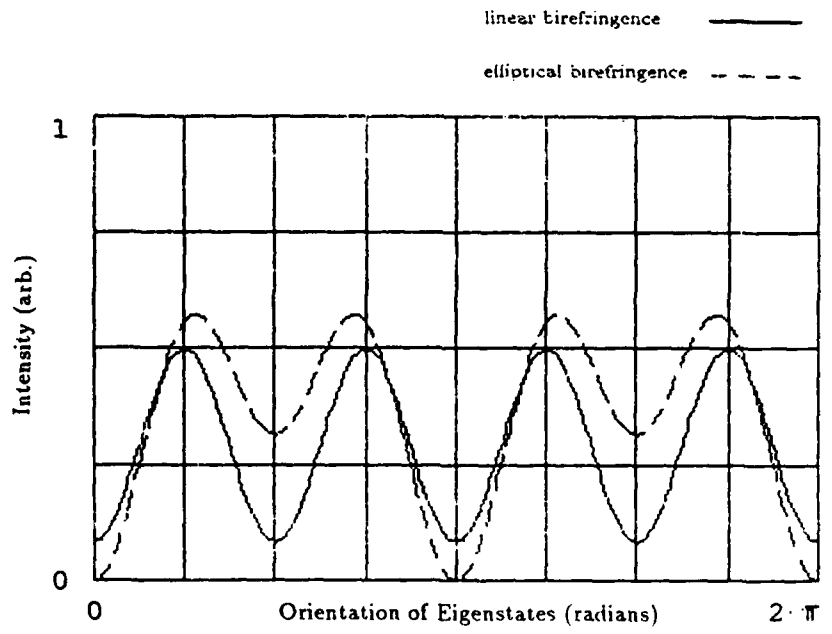

Figure 43. Intensity for $\xi = \pi/2$ and $\rho = \pi/4.5$

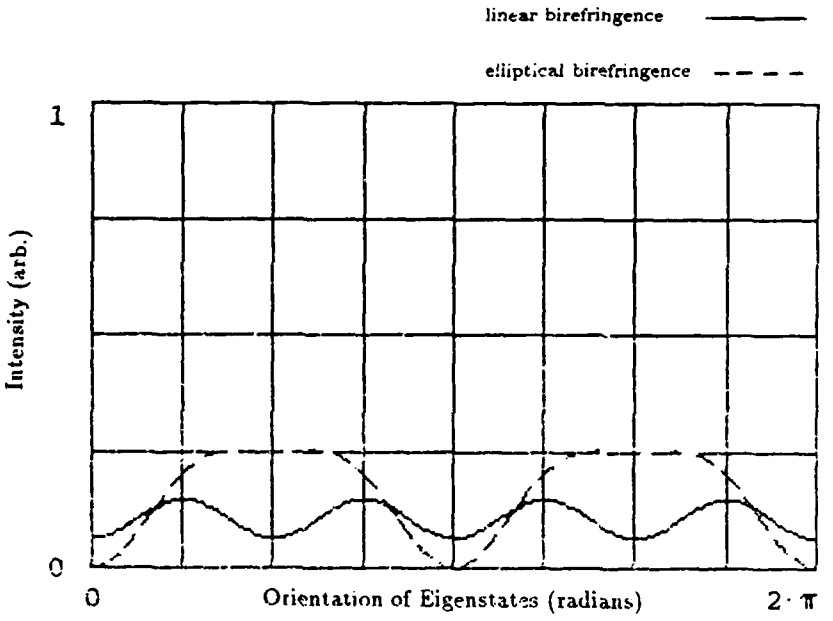

Figure 44. Intensity for $\xi = \pi/4$ and $\rho = \pi/4.5$

Bibliography

1. Abrahams, S.C. *et al.* "Crystal Chirality and Optical Rotation Sense in Isomorphous $Bi_{12}SiO_{20}$ and $Bi_{12}GeO_{20}$," *Solid State Communications*, 30: 293–295 (May 1979).

2. Casasent, D. *et al.* "Applications of the PRIZ Light Modulator," *Applied Optics*, 21: 3846–3854 (November 1982).

3. Gardner, Capt Patrick. *Evaluation of the Spatial and Temporal Characteristics of the Conducting PRIZ.* MS thesis, AFIT/GEO/ENP/88D-2. School of Engineering, Air Force Institute of Technology (AU), Wright-Patterson AFB OH, December 1988.

4. Günter, P. "Holography, Coherent Light Amplification and Optical Phase Conjugation with Photorefractive Materials," *Physics Reports*, 93: 199–299 (1982).

5. Hecht, Eugene. *Optics* (Second Edition). Reading MA: Addison-Wesley Publishing Company, 1987.

6. Jones, R. Clark. "A New Calculus for the Treatment of Optical Systems. VII. Properties of the N-Matrices," *Journal of the Optical Society of America*, 38: 671–685 (August 1948).

7. Juretschke, Hellmut J. *Crystal Physics.* Reading MA: W.A. Benjamin, Inc., 1974.

8. Nye, J.F. *Physical Properties of Crystals.* New York: Oxford at the Clarendon Press, 1957.

9. Owechko, Y. and A.R. Tanguay, Jr. "Theoretical Resolution Limitations of Electrooptic Spatial Light Modulators. II. Effects of Crystallographic Orientation," *Journal of the Optical Society of America*, A1: 644–652 (June 1984).

10. Pellat-Finet, Pierre and Guy Lebreton. "Electro-optical Coefficient in BSO-Type Crystals with Optical Activity: Measurement and Applications," *Proceedings of SPIE — The International Society for Optical Engineering*, 400: 151–158. Geneva, Switzerland: April 20–21, 1983.

11. Petrov, M.P. *et al.* "The PRIZ Image Converter and Its Use in Optical Data Processing Systems," *Soviet Physics Technical Physics*, 26: 816–821 (July 1981).

12. Petrov, M.P. and A.V. Khomenko. "Anisotropy of the Photorefractive Effect in $Bi_{12}SiO_{20}$ Crystals," *Soviet Physics Solid State*, 23: 789–792 (May 1981).

13. Ramachandran, G.N. and S. Ramaseshan. "Crystal Optics," *Encyclopedia of Physics*, Volume XXV/1, edited by S. Flügge. Berlin: Springer-Verlag, 1961.

14. Shurcliff, William A. *Polarized Light.* Cambridge MA: Harvard University Press, 1962.

15. Tanguay, A.R., Jr. *Czochralski Growth and Optical Properties of Bismuth Silicon Oxide.* PhD dissertation. Yale University, New Haven CT, 1977.

16. Yariv, Amnon and Pochi Yeh. *Optical Waves in Crystals.* New York: John Wiley & Sons, Inc., 1984.

Vita

Captain Richard J. Padden [redacted] He attended Worcester Polytechnic Institute in Massachusetts, where he earned the degree of Bachelor of Science in Electrical Engineering. He entered military service through the Air Force College Senior Engineering Program, and was commissioned at Officers Training School in September, 1983. His first assignment was as an Avionics Systems Engineer for Aeronautical Systems Division, Wright-Patterson AFB. He entered the School of Engineering, Air Force Institute of Technology, in May 1987.

[redacted]

UNCLASSIFIED

SECURITY CLASSIFICATION OF THIS PAGE

ADA202530

REPORT DOCUMENTATION PAGE

Form Approved OMB No. 0704-0188

1a. REPORT SECURITY CLASSIFICATION: Unclassified	1b. RESTRICTIVE MARKINGS
2a. SECURITY CLASSIFICATION AUTHORITY	3. DISTRIBUTION/AVAILABILITY OF REPORT: Approved for public release; distribution unlimited.
2b. DECLASSIFICATION/DOWNGRADING SCHEDULE	
4. PERFORMING ORGANIZATION REPORT NUMBER(S): AFIT/GEO/ENP/88D-4	5. MONITORING ORGANIZATION REPORT NUMBER(S)
6a. NAME OF PERFORMING ORGANIZATION: School of Engineering; 6b. OFFICE SYMBOL (If applicable): AFIT/ENP	7a. NAME OF MONITORING ORGANIZATION
6c. ADDRESS (City, State, and ZIP Code): Air Force Institute of Technology (AU) Wright-Patterson AFB, Ohio 45433-6583	7b. ADDRESS (City, State, and ZIP Code)
8a. NAME OF FUNDING/SPONSORING ORGANIZATION; 8b. OFFICE SYMBOL (If applicable)	9. PROCUREMENT INSTRUMENT IDENTIFICATION NUMBER
8c. ADDRESS (City, State, and ZIP Code)	10. SOURCE OF FUNDING NUMBERS: PROGRAM ELEMENT NO. / PROJECT NO. / TASK NO / WORK UNIT ACCESSION NO.

Approved for release in accordance with AFR 190-1
12 Jan 1989

11. TITLE (Include Security Classification)

OPTICAL ACTIVITY AND ITS INFLUENCE ON PHOTOREFRACTIVE MATERIALS

12. PERSONAL AUTHOR(S)
Richard J. Padden, Capt, USAF

13a. TYPE OF REPORT	13b. TIME COVERED	14. DATE OF REPORT (Year, Month, Day)	15. PAGE COUNT
MS Thesis	FROM _____ TO _____	1988, December	79

16. SUPPLEMENTARY NOTATION

17. COSATI CODES			18. SUBJECT TERMS (Continue on reverse if necessary and identify by block number)
FIELD	GROUP	SUB-GROUP	Optical Activity; Elliptical Birefringence; Photorefractive Materials; BSO; PRIZ
20	06		

19. ABSTRACT (Continue on reverse if necessary and identify by block number)

Thesis Advisor: Dr. T.E. Luke
Professor of Engineering Physics

This study characterized the effect of optical activity on the input-output properties of a photorefractive material. Optical activity is a material that causes incident linearly polarized light to rotate as it travels through a crystal. The photorefractive effect causes a linear birefringence to develop in the crystal as a result of photoconductivity and the linear electro-optic effect. The combination of optical activity and linear birefringence was investigated using two consistent representations: the Poincare sphere and Jones matrices. The results showed that the combination of the two effects is a nonlinear superposition which results in an elliptically birefringent crystal.

(continued on reverse)

20. DISTRIBUTION/AVAILABILITY OF ABSTRACT: ☒ UNCLASSIFIED/UNLIMITED ☐ SAME AS RPT. ☐ DTIC USERS	21. ABSTRACT SECURITY CLASSIFICATION: Unclassified
22a. NAME OF RESPONSIBLE INDIVIDUAL: Theodore E. Luke, Professor	22b. TELEPHONE (Include Area Code): (513) 255-4498; 22c. OFFICE SYMBOL: AFIT/ENP

DD Form 1473, JUN 86 — Previous editions are obsolete.

SECURITY CLASSIFICATION OF THIS PAGE
UNCLASSIFIED

19. (cont'd)

The two representations were used to investigate the effects of optical activity in an imaging device called the PRIZ, which uses the optically active, photorefractive crystal BSO. The orientation of the eigenstates of the (111) PRIZ investigated are dependent on the direction, but not the magnitude, of the internal transverse electric field. Conversely, the amount of linear birefringence is dependent on only the magnitude of this field. Analysis of the input-output characteristics showed that for small values of linear birefringence close to the value of optical activity, the output intensity for elliptical birefringence was noticeably different from that of linear birefringence. Results also showed that elliptical input polarization exhibited directional filtering similar to that already reported for linear polarization, while circular input did not.

Trials were also run using the laboratory configuration of an analyzer biased to compensate for the optical rotation. The results showed that both linear and elliptical birefringence exhibited directional filtering and an asymmetric output intensity. The conclusions drawn from these results were that for the PRIZ imaging device, circular read beam input polarization is the best to use because it causes no directional filtering. Also, for the PRIZ application of BSO discussed, the effects of optical activity result in a minor deviation from the case considering only the linear birefringence response. The recommendations from this study are to use circular input polarization for better imaging quality, and investigate other materials and applications involving optical activity.